

# Aerodynamic Shape Optimization Using the Adjoint Method

Antony Jameson

Department of Aeronautics & Astronautics  
Stanford University  
Stanford, California 94305 USA

Lectures at the Von Karman Institute, Brussels  
February 6, 2003

## Abstract

These Lecture Notes review the formulation and application of optimization techniques based on control theory for aerodynamic shape design in both inviscid and viscous compressible flow. The theory is applied to a system defined by the partial differential equations of the flow, with the boundary shape acting as the control. The Frechet derivative of the cost function is determined via the solution of an adjoint partial differential equation, and the boundary shape is then modified in a direction of descent. This process is repeated until an optimum solution is approached. Each design cycle requires the numerical solution of both the flow and the adjoint equations, leading to a computational cost roughly equal to the cost of two flow solutions. Representative results are presented for viscous optimization of transonic wing-body combinations.

## 1 Introduction: Aerodynamic Design

The definition of the aerodynamic shapes of modern aircraft relies heavily on computational simulation to enable the rapid evaluation of many alternative designs. Wind tunnel testing is then used to confirm the performance of designs that have been identified by simulation as promising to meet the performance goals. In the case of wing design and propulsion system integration, several complete cycles of computational analysis followed by testing of a preferred design may be used in the evolution of the final configuration. Wind tunnel testing also plays a crucial role in the development of the detailed loads needed to complete the structural design, and in gathering data throughout the flight envelope for the design and verification of the stability and control system. The use of computational simulation to scan many alternative designs has proved extremely valuable in practice, but it still suffers the limitation that it does not guarantee the identification of the best possible design. Generally one has to accept the best so far by a given cutoff date in the program schedule. To ensure the realization of the true best design, the ultimate goal of computational simulation methods should not just be the analysis of prescribed shapes, but the automatic determination of the true optimum shape for the intended application.

This is the underlying motivation for the combination of computational fluid dynamics with numerical optimization methods. Some of the earliest studies of such an approach were made by Hicks and Henne [1,2]. The principal obstacle was the large computational cost of determining the sensitivity of the cost function to variations of the design parameters by repeated calculation of the flow. Another way to approach the problem is to formulate aerodynamic shape design within the framework of the mathematical theory for the control of systems governed by partial differential equations [3]. In this view the wing is regarded as a device to produce lift by controlling the flow, and its design is regarded as a problem in the optimal control of the flow equations by changing the shape of the boundary. If the boundary shape is regarded as arbitrary within some requirements of smoothness, then the full generality of shapes cannot be defined with a finite number of parameters, and one must use the concept of the Frechet derivative of the cost with respect to a function. Clearly such a derivative cannot be determined directly by separate variation of each design parameter, because there are now an infinite number of these.

Using techniques of control theory, however, the gradient can be determined indirectly by solving an adjoint equation which has coefficients determined by the solution of the flow equations. This directly corresponds to the gradient technique for trajectory optimization pioneered by Bryson [4]. The cost of solving

the adjoint equation is comparable to the cost of solving the flow equations, with the consequence that the gradient with respect to an arbitrarily large number of parameters can be calculated with roughly the same computational cost as two flow solutions. Once the gradient has been calculated, a descent method can be used to determine a shape change which will make an improvement in the design. The gradient can then be recalculated, and the whole process can be repeated until the design converges to an optimum solution, usually within 10 - 50 cycles. The fast calculation of the gradients makes optimization computationally feasible even for designs in three-dimensional viscous flow. There is a possibility that the descent method could converge to a local minimum rather than the global optimum solution. In practice this has not proved a difficulty, provided care is taken in the choice of a cost function which properly reflects the design requirements. Conceptually, with this approach the problem is viewed as infinitely dimensional, with the control being the shape of the bounding surface. Eventually the equations must be discretized for a numerical implementation of the method. For this purpose the flow and adjoint equations may either be separately discretized from their representations as differential equations, or, alternatively, the flow equations may be discretized first, and the discrete adjoint equations then derived directly from the discrete flow equations.

The effectiveness of optimization as a tool for aerodynamic design also depends crucially on the proper choice of cost functions and constraints. One popular approach is to define a target pressure distribution, and then solve the inverse problem of finding the shape that will produce that pressure distribution. Since such a shape does not necessarily exist, direct inverse methods may be ill-posed. The problem of designing a two-dimensional profile to attain a desired pressure distribution was studied by Lighthill, who solved it for the case of incompressible flow with a conformal mapping of the profile to a unit circle [5]. The speed over the profile is

$$q = \frac{1}{h} |\nabla\phi|,$$

where  $\phi$  is the potential which is known for incompressible flow and  $h$  is the modulus of the mapping function. The surface value of  $h$  can be obtained by setting  $q = q_d$ , where  $q_d$  is the desired speed, and since the mapping function is analytic, it is uniquely determined by the value of  $h$  on the boundary. A solution exists for a given speed  $q_\infty$  at infinity only if

$$\frac{1}{2\pi} \oint q d\theta = q_\infty,$$

and there are additional constraints on  $q$  if the profile is required to be closed.

The difficulty that the target pressure may be unattainable may be circumvented by treating the inverse problem as a special case of the optimization problem, with a cost function which measures the error in the solution of the inverse problem. For example, if  $p_d$  is the desired surface pressure, one may take the cost function to be an integral over the the body surface of the square of the pressure error,

$$I = \frac{1}{2} \int_{\mathcal{B}} (p - p_d)^2 d\mathcal{B},$$

or possibly a more general Sobolev norm of the pressure error. This has the advantage of converting a possibly ill posed problem into a well posed one. It has the disadvantage that it incurs the computational costs associated with optimization procedures.

The inverse problem still leaves the definition of an appropriate pressure architecture to the designer. One may prefer to directly improve suitable performance parameters, for example, to minimize the drag at a given lift and Mach number. In this case it is important to introduce appropriate constraints. For example, if the span is not fixed the vortex drag can be made arbitrarily small by sufficiently increasing the span. In practice, a useful approach is to fix the planform, and optimize the wing sections subject to constraints on minimum thickness.

Studies of the use of control theory for optimum shape design of systems governed by elliptic equations were initiated by Pironneau [6]. The control theory approach to optimal aerodynamic design was first applied to transonic flow by Jameson [7–12]. He formulated the method for inviscid compressible flows with shock waves governed by both the potential flow and the Euler equations [8]. Numerical results showing the method to be extremely effective for the design of airfoils in transonic potential flow were presented in [13,14], and for three-dimensional wing design using the Euler equations in [15]. More recently the method has been employed for the shape design of complex aircraft configurations [16,17], using a grid perturbation approach to accommodate the geometry modifications. The method has been used to support the aerodynamic design

studies of several industrial projects, including the Beech Premier and the McDonnell Douglas MDXX and Blended Wing-Body projects. The application to the MDXX is described in [10]. The experience gained in these industrial applications made it clear that the viscous effects cannot be ignored in transonic wing design, and the method has therefore been extended to treat the Reynolds Averaged Navier-Stokes equations [12]. Adjoint methods have also been the subject of studies by a number of other authors, including Baysal and Eleshaky [18], Huan and Modi [19], Desai and Ito [20], Anderson and Venkatakrishnan [21], and Peraire and Elliot [22]. Ta'asan, Kuruvila and Salas [23], who have implemented a one shot approach in which the constraint represented by the flow equations is only required to be satisfied by the final converged solution. In their work, computational costs are also reduced by applying multigrid techniques to the geometry modifications as well as the solution of the flow and adjoint equations.

## 2 Formulation of the Design Problem as a Control Problem

The simplest approach to optimization is to define the geometry through a set of design parameters, which may, for example, be the weights  $\alpha_i$  applied to a set of shape functions  $b_i(x)$  so that the shape is represented as

$$f(x) = \sum \alpha_i b_i(x).$$

Then a cost function  $I$  is selected which might, for example, be the drag coefficient or the lift to drag ratio, and  $I$  is regarded as a function of the parameters  $\alpha_i$ . The sensitivities  $\frac{\partial I}{\partial \alpha_i}$  may now be estimated by making a small variation  $\delta \alpha_i$  in each design parameter in turn and recalculating the flow to obtain the change in  $I$ . Then

$$\frac{\partial I}{\partial \alpha_i} \approx \frac{I(\alpha_i + \delta \alpha_i) - I(\alpha_i)}{\delta \alpha_i}.$$

The gradient vector  $\frac{\partial I}{\partial \alpha}$  may now be used to determine a direction of improvement. The simplest procedure is to make a step in the negative gradient direction by setting

$$\alpha^{n+1} = \alpha^n - \lambda \delta \alpha,$$

so that to first order

$$I + \delta I = I - \frac{\partial I^T}{\partial \alpha} \delta \alpha = I - \lambda \frac{\partial I^T}{\partial \alpha} \frac{\partial I}{\partial \alpha}.$$

More sophisticated search procedures may be used such as quasi-Newton methods, which attempt to estimate the second derivative  $\frac{\partial^2 I}{\partial \alpha_i \partial \alpha_j}$  of the cost function from changes in the gradient  $\frac{\partial I}{\partial \alpha}$  in successive optimization steps. These methods also generally introduce line searches to find the minimum in the search direction which is defined at each step. The main disadvantage of this approach is the need for a number of flow calculations proportional to the number of design variables to estimate the gradient. The computational costs can thus become prohibitive as the number of design variables is increased.

Using techniques of control theory, however, the gradient can be determined indirectly by solving an adjoint equation which has coefficients defined by the solution of the flow equations. The cost of solving the adjoint equation is comparable to that of solving the flow equations. Thus the gradient can be determined with roughly the computational costs of two flow solutions, independently of the number of design variables, which may be infinite if the boundary is regarded as a free surface. The underlying concepts are clarified by the following abstract description of the adjoint method.

For flow about an airfoil or wing, the aerodynamic properties which define the cost function are functions of the flow-field variables ( $w$ ) and the physical location of the boundary, which may be represented by the function  $\mathcal{F}$ , say. Then

$$I = I(w, \mathcal{F}),$$

and a change in  $\mathcal{F}$  results in a change

$$\delta I = \left[ \frac{\partial I^T}{\partial w} \right]_I \delta w + \left[ \frac{\partial I^T}{\partial \mathcal{F}} \right]_{II} \delta \mathcal{F} \quad (1)$$

in the cost function. Here, the subscripts  $I$  and  $II$  are used to distinguish the contributions due to the variation  $\delta w$  in the flow solution from the change associated directly with the modification  $\delta \mathcal{F}$  in the shape.

This notation assists in grouping the numerous terms that arise during the derivation of the full Navier–Stokes adjoint operator, outlined later, so that the basic structure of the approach as it is sketched in the present section can easily be recognized.

Suppose that the governing equation  $R$  which expresses the dependence of  $w$  and  $\mathcal{F}$  within the flowfield domain  $D$  can be written as

$$R(w, \mathcal{F}) = 0. \quad (2)$$

Then  $\delta w$  is determined from the equation

$$\delta R = \left[ \frac{\partial R}{\partial w} \right]_I \delta w + \left[ \frac{\partial R}{\partial \mathcal{F}} \right]_{II} \delta \mathcal{F} = 0. \quad (3)$$

Since the variation  $\delta R$  is zero, it can be multiplied by a Lagrange Multiplier  $\psi$  and subtracted from the variation  $\delta I$  without changing the result. Thus equation (1) can be replaced by

$$\begin{aligned} \delta I &= \frac{\partial I^T}{\partial w} \delta w + \frac{\partial I^T}{\partial \mathcal{F}} \delta \mathcal{F} - \psi^T \left( \left[ \frac{\partial R}{\partial w} \right] \delta w + \left[ \frac{\partial R}{\partial \mathcal{F}} \right] \delta \mathcal{F} \right) \\ &= \left\{ \frac{\partial I^T}{\partial w} - \psi^T \left[ \frac{\partial R}{\partial w} \right] \right\}_I \delta w + \left\{ \frac{\partial I^T}{\partial \mathcal{F}} - \psi^T \left[ \frac{\partial R}{\partial \mathcal{F}} \right] \right\}_{II} \delta \mathcal{F}. \end{aligned} \quad (4)$$

Choosing  $\psi$  to satisfy the adjoint equation

$$\left[ \frac{\partial R}{\partial w} \right]^T \psi = \frac{\partial I}{\partial w} \quad (5)$$

the first term is eliminated, and we find that

$$\delta I = \mathcal{G} \delta \mathcal{F}, \quad (6)$$

where

$$\mathcal{G} = \frac{\partial I^T}{\partial \mathcal{F}} - \psi^T \left[ \frac{\partial R}{\partial \mathcal{F}} \right].$$

The advantage is that (6) is independent of  $\delta w$ , with the result that the gradient of  $I$  with respect to an arbitrary number of design variables can be determined without the need for additional flow-field evaluations. In the case that (2) is a partial differential equation, the adjoint equation (5) is also a partial differential equation and determination of the appropriate boundary conditions requires careful mathematical treatment.

In reference [8] Jameson derived the adjoint equations for transonic flows modeled by both the potential flow equation and the Euler equations. The theory was developed in terms of partial differential equations, leading to an adjoint partial differential equation. In order to obtain numerical solutions both the flow and the adjoint equations must be discretized. Control theory might be applied directly to the discrete flow equations which result from the numerical approximation of the flow equations by finite element, finite volume or finite difference procedures. This leads directly to a set of discrete adjoint equations with a matrix which is the transpose of the Jacobian matrix of the full set of discrete nonlinear flow equations. On a three-dimensional mesh with indices  $i, j, k$  the individual adjoint equations may be derived by collecting together all the terms multiplied by the variation  $\delta w_{i,j,k}$  of the discrete flow variable  $w_{i,j,k}$ . The resulting discrete adjoint equations represent a possible discretization of the adjoint partial differential equation. If these equations are solved exactly they can provide an exact gradient of the inexact cost function which results from the discretization of the flow equations. The discrete adjoint equations derived directly from the discrete flow equations become very complicated when the flow equations are discretized with higher order upwind biased schemes using flux limiters. On the other hand any consistent discretization of the adjoint partial differential equation will yield the exact gradient in the limit as the mesh is refined. The trade-off between the complexity of the adjoint discretization, the accuracy of the resulting estimate of the gradient, and its impact on the computational cost to approach an optimum solution is a subject of ongoing research.

The true optimum shape belongs to an infinitely dimensional space of design parameters. One motivation for developing the theory for the partial differential equations of the flow is to provide an indication in

principle of how such a solution could be approached if sufficient computational resources were available. It displays the character of the adjoint equation as a hyperbolic system with waves travelling in the reverse direction to those of the flow equations, and the need for correct wall and far-field boundary conditions. It also highlights the possibility of generating ill posed formulations of the problem. For example, if one attempts to calculate the sensitivity of the pressure at a particular location to changes in the boundary shape, there is the possibility that a shape modification could cause a shock wave to pass over that location. Then the sensitivity could become unbounded. The movement of the shock, however, is continuous as the shape changes. Therefore a quantity such as the drag coefficient, which is determined by integrating the pressure over the surface, also depends continuously on the shape. The adjoint equation allows the sensitivity of the drag coefficient to be determined without the explicit evaluation of pressure sensitivities which would be ill posed. Another benefit of the continuous adjoint formulation is that it allows grid sensitivity terms to be eliminated from the gradient, which can finally be expressed purely in terms of the boundary displacement, as will be shown in Section 4. This greatly simplifies the implementation of the method for overset or unstructured grids.

The discrete adjoint equations, whether they are derived directly or by discretization of the adjoint partial differential equation, are linear. Therefore they could be solved by direct numerical inversion. In three-dimensional problems on a mesh with, say,  $n$  intervals in each coordinate direction, the number of unknowns is proportional to  $n^3$  and the bandwidth to  $n^2$ . The complexity of direct inversion is proportional to the number of unknowns multiplied by the square of the bandwidth, resulting in a complexity proportional to  $n^7$ . The cost of direct inversion can thus become prohibitive as the mesh is refined, and it becomes more efficient to use iterative solution methods. Moreover, because of the similarity of the adjoint equations to the flow equations, the same iterative methods which have been proved to be efficient for the solution of the flow equations are efficient for the solution of the adjoint equations.

### 3 Design using the Euler Equations

The application of control theory to aerodynamic design problems is illustrated in this section for the case of three-dimensional wing design using the compressible Euler equations as the mathematical model. It proves convenient to denote the Cartesian coordinates and velocity components by  $x_1, x_2, x_3$  and  $u_1, u_2, u_3$ , and to use the convention that summation over  $i = 1$  to 3 is implied by a repeated index  $i$ . Then, the three-dimensional Euler equations may be written as

$$\frac{\partial w}{\partial t} + \frac{\partial f_i}{\partial x_i} = 0 \quad \text{in } D, \quad (7)$$

where

$$w = \begin{pmatrix} \rho \\ \rho u_1 \\ \rho u_2 \\ \rho u_3 \\ \rho E \end{pmatrix}, \quad f_i = \begin{pmatrix} \rho u_i \\ \rho u_i u_1 + p \delta_{i1} \\ \rho u_i u_2 + p \delta_{i2} \\ \rho u_i u_3 + p \delta_{i3} \\ \rho u_i H \end{pmatrix} \quad (8)$$

and  $\delta_{ij}$  is the Kronecker delta function. Also,

$$p = (\gamma - 1) \rho \left\{ E - \frac{1}{2} (u_i^2) \right\}, \quad (9)$$

and

$$\rho H = \rho E + p \quad (10)$$

where  $\gamma$  is the ratio of the specific heats.

In order to simplify the derivation of the adjoint equations, we map the solution to a fixed computational domain with coordinates  $\xi_1, \xi_2, \xi_3$  where

$$K_{ij} = \left[ \frac{\partial x_i}{\partial \xi_j} \right], \quad J = \det(K), \quad K_{ij}^{-1} = \left[ \frac{\partial \xi_i}{\partial x_j} \right],$$

and

$$S = JK^{-1}.$$

The elements of  $S$  are the cofactors of  $K$ , and in a finite volume discretization they are just the face areas of the computational cells projected in the  $x_1$ ,  $x_2$ , and  $x_3$  directions. Using the permutation tensor  $\epsilon_{ijk}$  we can express the elements of  $S$  as

$$S_{ij} = \frac{1}{2} \epsilon_{jpr} \epsilon_{irs} \frac{\partial x_p}{\partial \xi_r} \frac{\partial x_q}{\partial \xi_s}. \quad (11)$$

Then

$$\begin{aligned} \frac{\partial}{\partial \xi_i} S_{ij} &= \frac{1}{2} \epsilon_{jpr} \epsilon_{irs} \left( \frac{\partial^2 x_p}{\partial \xi_r \partial \xi_i} \frac{\partial x_q}{\partial \xi_s} + \frac{\partial x_p}{\partial \xi_r} \frac{\partial^2 x_q}{\partial \xi_s \partial \xi_i} \right) \\ &= 0. \end{aligned} \quad (12)$$

Also in the subsequent analysis of the effect of a shape variation it is useful to note that

$$\begin{aligned} S_{1j} &= \epsilon_{jpr} \frac{\partial x_p}{\partial \xi_2} \frac{\partial x_q}{\partial \xi_3}, \\ S_{2j} &= \epsilon_{jpr} \frac{\partial x_p}{\partial \xi_3} \frac{\partial x_q}{\partial \xi_1}, \\ S_{3j} &= \epsilon_{jpr} \frac{\partial x_p}{\partial \xi_1} \frac{\partial x_q}{\partial \xi_2}. \end{aligned} \quad (13)$$

Now, multiplying equation(7) by  $J$  and applying the chain rule,

$$J \frac{\partial w}{\partial t} + R(w) = 0 \quad (14)$$

where

$$R(w) = S_{ij} \frac{\partial f_j}{\partial \xi_i} = \frac{\partial}{\partial \xi_i} (S_{ij} f_j), \quad (15)$$

using (12). We can write the transformed fluxes in terms of the scaled contravariant velocity components

$$U_i = S_{ij} u_j$$

as

$$F_i = S_{ij} f_j = \begin{bmatrix} \rho U_i \\ \rho U_i u_1 + S_{i1} p \\ \rho U_i u_2 + S_{i2} p \\ \rho U_i u_3 + S_{i3} p \\ \rho U_i H \end{bmatrix}.$$

For convenience, the coordinates  $\xi_i$  describing the fixed computational domain are chosen so that each boundary conforms to a constant value of one of these coordinates. Variations in the shape then result in corresponding variations in the mapping derivatives defined by  $K_{ij}$ . Suppose that the performance is measured by a cost function

$$I = \int_{\mathcal{B}} \mathcal{M}(w, S) dB_{\xi} + \int_{\mathcal{D}} \mathcal{P}(w, S) dD_{\xi},$$

containing both boundary and field contributions where  $dB_{\xi}$  and  $dD_{\xi}$  are the surface and volume elements in the computational domain. In general,  $\mathcal{M}$  and  $\mathcal{P}$  will depend on both the flow variables  $w$  and the metrics  $S$  defining the computational space. The design problem is now treated as a control problem where the boundary shape represents the control function, which is chosen to minimize  $I$  subject to the constraints defined by the flow equations (14). A shape change produces a variation in the flow solution  $\delta w$  and the metrics  $\delta S$  which in turn produce a variation in the cost function

$$\delta I = \int_{\mathcal{B}} \delta \mathcal{M}(w, S) dB_{\xi} + \int_{\mathcal{D}} \delta \mathcal{P}(w, S) dD_{\xi}. \quad (16)$$

This can be split as

$$\delta I = \delta I_I + \delta I_{II}, \quad (17)$$

with

$$\begin{aligned} \delta \mathcal{M} &= [\mathcal{M}_w]_I \delta w + \delta \mathcal{M}_{II}, \\ \delta \mathcal{P} &= [\mathcal{P}_w]_I \delta w + \delta \mathcal{P}_{II}, \end{aligned} \quad (18)$$

where we continue to use the subscripts  $I$  and  $II$  to distinguish between the contributions associated with the variation of the flow solution  $\delta w$  and those associated with the metric variations  $\delta S$ . Thus  $[\mathcal{M}_w]_I$  and  $[\mathcal{P}_w]_I$  represent  $\frac{\partial \mathcal{M}}{\partial w}$  and  $\frac{\partial \mathcal{P}}{\partial w}$  with the metrics fixed, while  $\delta \mathcal{M}_{II}$  and  $\delta \mathcal{P}_{II}$  represent the contribution of the metric variations  $\delta S$  to  $\delta \mathcal{M}$  and  $\delta \mathcal{P}$ .

In the steady state, the constraint equation (14) specifies the variation of the state vector  $\delta w$  by

$$\delta R = \frac{\partial}{\partial \xi_i} \delta F_i = 0. \quad (19)$$

Here also,  $\delta R$  and  $\delta F_i$  can be split into contributions associated with  $\delta w$  and  $\delta S$  using the notation

$$\begin{aligned} \delta R &= \delta R_I + \delta R_{II} \\ \delta F_i &= [F_{iw}]_I \delta w + \delta F_{iII}. \end{aligned} \quad (20)$$

where

$$[F_{iw}]_I = S_{ij} \frac{\partial f_i}{\partial w}.$$

Multiplying by a co-state vector  $\psi$ , which will play an analogous role to the Lagrange multiplier introduced in equation (4), and integrating over the domain produces

$$\int_{\mathcal{D}} \psi^T \frac{\partial}{\partial \xi_i} \delta F_i d\mathcal{D}_\xi = 0. \quad (21)$$

Assuming that  $\psi$  is differentiable, the terms with subscript  $I$  may be integrated by parts to give

$$\int_{\mathcal{B}} n_i \psi^T \delta F_{iI} d\mathcal{B}_\xi - \int_{\mathcal{D}} \frac{\partial \psi^T}{\partial \xi_i} \delta F_{iI} d\mathcal{D}_\xi + \int_{\mathcal{D}} \psi^T \delta R_{II} d\mathcal{D}_\xi = 0. \quad (22)$$

This equation results directly from taking the variation of the weak form of the flow equations, where  $\psi$  is taken to be an arbitrary differentiable test function. Since the left hand expression equals zero, it may be subtracted from the variation in the cost function (16) to give

$$\begin{aligned} \delta I &= \delta I_{II} - \int_{\mathcal{D}} \psi^T \delta R_{II} d\mathcal{D}_\xi - \int_{\mathcal{B}} [\delta \mathcal{M}_I - n_i \psi^T \delta F_{iI}] d\mathcal{B}_\xi \\ &\quad + \int_{\mathcal{D}} \left[ \delta \mathcal{P}_I + \frac{\partial \psi^T}{\partial \xi_i} \delta F_{iI} \right] d\mathcal{D}_\xi. \end{aligned} \quad (23)$$

Now, since  $\psi$  is an arbitrary differentiable function, it may be chosen in such a way that  $\delta I$  no longer depends explicitly on the variation of the state vector  $\delta w$ . The gradient of the cost function can then be evaluated directly from the metric variations without having to recompute the variation  $\delta w$  resulting from the perturbation of each design variable.

Comparing equations (18) and (20), the variation  $\delta w$  may be eliminated from (23) by equating all field terms with subscript “ $I$ ” to produce a differential adjoint system governing  $\psi$

$$\frac{\partial \psi^T}{\partial \xi_i} [F_{iw}]_I + [\mathcal{P}_w]_I = 0 \quad \text{in } \mathcal{D}. \quad (24)$$

Taking the transpose of equation (24), in the case that there is no field integral in the cost function, the inviscid adjoint equation may be written as

$$C_i^T \frac{\partial \psi}{\partial \xi_i} = 0 \quad \text{in } \mathcal{D}, \quad (25)$$

where the inviscid Jacobian matrices in the transformed space are given by

$$C_i = S_{ij} \frac{\partial f_j}{\partial w}.$$

The corresponding adjoint boundary condition is produced by equating the subscript “ $I$ ” boundary terms in equation (23) to produce

$$n_i \psi^T [F_{iw}]_I = [\mathcal{M}_w]_I \quad \text{on } \mathcal{B}. \quad (26)$$

The remaining terms from equation (23) then yield a simplified expression for the variation of the cost function which defines the gradient

$$\delta I = \delta I_{II} + \int_{\mathcal{D}} \psi^T \delta R_{II} d\mathcal{D}_\xi, \quad (27)$$

which consists purely of the terms containing variations in the metrics, with the flow solution fixed. Hence an explicit formula for the gradient can be derived once the relationship between mesh perturbations and shape variations is defined.

The details of the formula for the gradient depend on the way in which the boundary shape is parameterized as a function of the design variables, and the way in which the mesh is deformed as the boundary is modified. Using the relationship between the mesh deformation and the surface modification, the field integral is reduced to a surface integral by integrating along the coordinate lines emanating from the surface. Thus the expression for  $\delta I$  is finally reduced to the form of equation (6)

$$\delta I = \int_{\mathcal{B}} \mathcal{G} \delta \mathcal{F} d\mathcal{B}_\xi$$

where  $\mathcal{F}$  represents the design variables, and  $\mathcal{G}$  is the gradient, which is a function defined over the boundary surface.

The boundary conditions satisfied by the flow equations restrict the form of the left hand side of the adjoint boundary condition (26). Consequently, the boundary contribution to the cost function  $\mathcal{M}$  cannot be specified arbitrarily. Instead, it must be chosen from the class of functions which allow cancellation of all terms containing  $\delta w$  in the boundary integral of equation (23). On the other hand, there is no such restriction on the specification of the field contribution to the cost function  $\mathcal{P}$ , since these terms may always be absorbed into the adjoint field equation (24) as source terms.

For simplicity, it will be assumed that the portion of the boundary that undergoes shape modifications is restricted to the coordinate surface  $\xi_2 = 0$ . Then equations (23) and (26) may be simplified by incorporating the conditions

$$n_1 = n_3 = 0, \quad n_2 = 1, \quad d\mathcal{B}_\xi = d\xi_1 d\xi_3,$$

so that only the variation  $\delta F_2$  needs to be considered at the wall boundary. The condition that there is no flow through the wall boundary at  $\xi_2 = 0$  is equivalent to

$$U_2 = 0,$$

so that

$$\delta U_2 = 0$$

when the boundary shape is modified. Consequently the variation of the inviscid flux at the boundary reduces to

$$\delta F_2 = \delta p \begin{Bmatrix} 0 \\ S_{21} \\ S_{22} \\ S_{23} \\ 0 \end{Bmatrix} + p \begin{Bmatrix} 0 \\ \delta S_{21} \\ \delta S_{22} \\ \delta S_{23} \\ 0 \end{Bmatrix}. \quad (28)$$

Since  $\delta F_2$  depends only on the pressure, it is now clear that the performance measure on the boundary  $\mathcal{M}(w, S)$  may only be a function of the pressure and metric terms. Otherwise, complete cancellation of the terms containing  $\delta w$  in the boundary integral would be impossible. One may, for example, include arbitrary measures of the forces and moments in the cost function, since these are functions of the surface pressure.

In order to design a shape which will lead to a desired pressure distribution, a natural choice is to set

$$I = \frac{1}{2} \int_{\mathcal{B}} (p - p_d)^2 dS$$

where  $p_d$  is the desired surface pressure, and the integral is evaluated over the actual surface area. In the computational domain this is transformed to

$$I = \frac{1}{2} \iint_{\mathcal{B}_w} (p - p_d)^2 |S_2| d\xi_1 d\xi_3,$$

where the quantity

$$|S_2| = \sqrt{S_{2j} S_{2j}}$$

denotes the face area corresponding to a unit element of face area in the computational domain. Now, to cancel the dependence of the boundary integral on  $\delta p$ , the adjoint boundary condition reduces to

$$\psi_j n_j = p - p_d \quad (29)$$

where  $n_j$  are the components of the surface normal

$$n_j = \frac{S_{2j}}{|S_2|}.$$

This amounts to a transpiration boundary condition on the co-state variables corresponding to the momentum components. Note that it imposes no restriction on the tangential component of  $\psi$  at the boundary.

We find finally that

$$\begin{aligned} \delta I = & - \int_{\mathcal{D}} \frac{\partial \psi^T}{\partial \xi_i} \delta S_{ij} f_j d\mathcal{D} \\ & - \iint_{\mathcal{B}_w} (\delta S_{21} \psi_2 + \delta S_{22} \psi_3 + \delta S_{23} \psi_4) p d\xi_1 d\xi_3. \end{aligned} \quad (30)$$

Here the expression for the cost variation depends on the mesh variations throughout the domain which appear in the field integral. However, the true gradient for a shape variation should not depend on the way in which the mesh is deformed, but only on the true flow solution. In the next section we show how the field integral can be eliminated to produce a reduced gradient formula which depends only on the boundary movement.

## 4 The Reduced Gradient Formulation

Consider the case of a mesh variation with a fixed boundary. Then,

$$\delta I = 0$$

but there is a variation in the transformed flux,

$$\delta F_i = C_i \delta w + \delta S_{ij} f_j.$$

Here the true solution is unchanged. Thus, the variation  $\delta w$  is due to the mesh movement  $\delta x$  at each mesh point. Therefore

$$\delta w = \nabla w \cdot \delta x = \frac{\partial w}{\partial x_j} \delta x_j (= \delta w^*)$$

and since

$$\frac{\partial}{\partial \xi_i} \delta F_i = 0,$$

it follows that

$$\frac{\partial}{\partial \xi_i} (\delta S_{ij} f_j) = -\frac{\partial}{\partial \xi_i} (C_i \delta w^*). \quad (31)$$

It is verified below that this relation holds in the general case with boundary movement. Now

$$\begin{aligned} \int_{\mathcal{D}} \phi^T \delta R d\mathcal{D} &= \int_{\mathcal{D}} \phi^T \frac{\partial}{\partial \xi_i} C_i (\delta w - \delta w^*) d\mathcal{D} \\ &= \int_{\mathcal{B}} \phi^T C_i (\delta w - \delta w^*) d\mathcal{B} \\ &\quad - \int_{\mathcal{D}} \frac{\partial \phi^T}{\partial \xi_i} C_i (\delta w - \delta w^*) d\mathcal{D}. \end{aligned} \quad (32)$$

Here on the wall boundary

$$C_2 \delta w = \delta F_2 - \delta S_{2j} f_j. \quad (33)$$

Thus, by choosing  $\phi$  to satisfy the adjoint equation (25) and the adjoint boundary condition (26), we reduce the cost variation to a boundary integral which depends only on the surface displacement:

$$\begin{aligned} \delta I &= \int_{\mathcal{B}_w} \psi^T (\delta S_{2j} f_j + C_2 \delta w^*) d\xi_1 d\xi_3 \\ &\quad - \int \int_{\mathcal{B}_w} (\delta S_{21} \psi_2 + \delta S_{22} \psi_3 + \delta S_{23} \psi_4) p d\xi_1 d\xi_3. \end{aligned} \quad (34)$$

For completeness the general derivation of equation(31) is presented here. Using the formula(11), and the property (12)

$$\begin{aligned} &\frac{\partial}{\partial \xi_i} (\delta S_{ij} f_j) \\ &= \frac{1}{2} \frac{\partial}{\partial \xi_i} \left\{ \epsilon_{j p q} \epsilon_{i r s} \left( \frac{\partial \delta x_p}{\partial \xi_r} \frac{\partial x_q}{\partial \xi_s} + \frac{\partial x_p}{\partial \xi_r} \frac{\partial \delta x_q}{\partial \xi_s} \right) f_j \right\} \\ &= \frac{1}{2} \epsilon_{j p q} \epsilon_{i r s} \left( \frac{\partial \delta x_p}{\partial \xi_r} \frac{\partial x_q}{\partial \xi_s} + \frac{\partial x_p}{\partial \xi_r} \frac{\partial \delta x_q}{\partial \xi_s} \right) \frac{\partial f_j}{\partial \xi_i} \\ &= \frac{1}{2} \epsilon_{j p q} \epsilon_{i r s} \left\{ \frac{\partial}{\partial \xi_r} \left( \delta x_p \frac{\partial x_q}{\partial \xi_s} \frac{\partial f_j}{\partial \xi_i} \right) \right\} \\ &\quad + \frac{1}{2} \epsilon_{j p q} \epsilon_{i r s} \left\{ \frac{\partial}{\partial \xi_s} \left( \delta x_q \frac{\partial x_p}{\partial \xi_r} \frac{\partial f_j}{\partial \xi_i} \right) \right\} \\ &= \frac{\partial}{\partial \xi_r} \left( \delta x_p \epsilon_{p q j} \epsilon_{r s i} \frac{\partial x_q}{\partial \xi_s} \frac{\partial f_j}{\partial \xi_i} \right). \end{aligned} \quad (35)$$

Now express  $\delta x_p$  in terms of a shift in the original computational coordinates

$$\delta x_p = \frac{\partial x_p}{\partial \xi_k} \delta \xi_k.$$

Then we obtain

$$\frac{\partial}{\partial \xi_i} (\delta S_{ij} f_j) = \frac{\partial}{\partial \xi_r} \left( \epsilon_{p q j} \epsilon_{r s i} \frac{\partial x_p}{\partial \xi_k} \frac{\partial x_q}{\partial \xi_s} \frac{\partial f_j}{\partial \xi_i} \delta \xi_k \right). \quad (36)$$

The term in  $\frac{\partial}{\partial \xi_1}$  is

$$\epsilon_{123} \epsilon_{p q j} \frac{\partial x_p}{\partial \xi_k} \left( \frac{\partial x_q}{\partial \xi_2} \frac{\partial f_j}{\partial \xi_3} - \frac{\partial x_q}{\partial \xi_3} \frac{\partial f_j}{\partial \xi_2} \right) \delta \xi_k.$$

Here the term multiplying  $\delta\xi_1$  is

$$\epsilon_{j pq} \left( \frac{\partial x_p}{\partial \xi_1} \frac{\partial x_q}{\partial \xi_2} \frac{\partial f_j}{\partial \xi_3} - \frac{\partial x_p}{\partial \xi_1} \frac{\partial x_q}{\partial \xi_3} \frac{\partial f_j}{\partial \xi_2} \right).$$

According to the formulas(13) this may be recognized as

$$S_{2j} \frac{\partial f_1}{\partial \xi_2} + S_{3j} \frac{\partial f_1}{\partial \xi_3}$$

or, using the quasi-linear form(15) of the equation for steady flow, as

$$-S_{1j} \frac{\partial f_1}{\partial \xi_1}.$$

The terms multiplying  $\delta\xi_2$  and  $\delta\xi_3$  are

$$\epsilon_{j pq} \left( \frac{\partial x_p}{\partial \xi_2} \frac{\partial x_q}{\partial \xi_2} \frac{\partial f_j}{\partial \xi_3} - \frac{\partial x_p}{\partial \xi_2} \frac{\partial x_q}{\partial \xi_3} \frac{\partial f_j}{\partial \xi_2} \right) = -S_{1j} \frac{\partial f_1}{\partial \xi_2}$$

and

$$\epsilon_{j pq} \left( \frac{\partial x_p}{\partial \xi_3} \frac{\partial x_q}{\partial \xi_2} \frac{\partial f_j}{\partial \xi_3} - \frac{\partial x_p}{\partial \xi_3} \frac{\partial x_q}{\partial \xi_3} \frac{\partial f_j}{\partial \xi_2} \right) = -S_{1j} \frac{\partial f_1}{\partial \xi_3}.$$

Thus the term in  $\frac{\partial}{\partial \xi_1}$  is reduced to

$$-\frac{\partial}{\partial \xi_1} \left( S_{1j} \frac{\partial f_1}{\partial \xi_k} \delta \xi_k \right).$$

Finally, with similar reductions of the terms in  $\frac{\partial}{\partial \xi_2}$  and  $\frac{\partial}{\partial \xi_3}$ , we obtain

$$\frac{\partial}{\partial \xi_i} (\delta S_{ij} f_j) = -\frac{\partial}{\partial \xi_i} \left( S_{ij} \frac{\partial f_j}{\partial \xi_k} \delta \xi_k \right) = -\frac{\partial}{\partial \xi_i} (C_i \delta w^*)$$

as was to be proved.

## 5 Optimization Procedure

### 5.1 The need for a Sobolev inner product in the definition of the gradient

Another key issue for successful implementation of the continuous adjoint method is the choice of an appropriate inner product for the definition of the gradient. It turns out that there is an enormous benefit from the use of a modified Sobolev gradient, which enables the generation of a sequence of smooth shapes. This can be illustrated by considering the simplest case of a problem in the calculus of variations.

Suppose that we wish to find the path  $y(x)$  which minimizes

$$I = \int_a^b F(y, y') dx$$

with fixed end points  $y(a)$  and  $y(b)$ . Under a variation  $\delta y(x)$ ,

$$\begin{aligned} \delta I &= \int_a^b \left( \frac{\partial F}{\partial y} \delta y + \frac{\partial F}{\partial y'} \delta y' \right) dx \\ &= \int_a^b \left( \frac{\partial F}{\partial y} - \frac{d}{dx} \frac{\partial F}{\partial y'} \right) \delta y dx \end{aligned}$$

Thus defining the gradient as

$$g = \frac{\partial F}{\partial y} - \frac{d}{dx} \frac{\partial F}{\partial y'}$$

and the inner product as

$$(u, v) = \int_a^b uv dx$$

we find that

$$\delta I = (g, \delta y).$$

If we now set

$$\delta y = -\lambda g, \quad \lambda > 0$$

we obtain a improvement

$$\delta I = -\lambda(g, g) \leq 0$$

unless  $g = 0$ , the necessary condition for a minimum.

Note that  $g$  is a function of  $y, y', y''$ ,

$$g = g(y, y', y'')$$

In the well known case of the Brachistrone problem, for example, which calls for the determination of the path of quickest descent between two laterally separated points when a particle falls under gravity,

$$F(y, y') = \sqrt{\frac{1 + y'^2}{y}}$$

and

$$g = -\frac{1 + y'^2 + 2yy''}{2(y(1 + y'^2))^{3/2}}$$

It can be seen that each step

$$y^{n+1} = y^n - \lambda^n g^n$$

reduces the smoothness of  $y$  by two classes. Thus the computed trajectory becomes less and less smooth, leading to instability.

In order to prevent this we can introduce a weighted Sobolev inner product [24]

$$\langle u, v \rangle = \int (uv + \epsilon u' v') dx$$

where  $\epsilon$  is a parameter that controls the weight of the derivatives. We now define a gradient  $\bar{g}$  such that

$$\delta I = \langle \bar{g}, \delta y \rangle$$

Then we have

$$\begin{aligned} \delta I &= \int (\bar{g} \delta y + \epsilon \bar{g}' \delta y') dx \\ &= \int \left( \bar{g} - \frac{\partial}{\partial x} \epsilon \frac{\partial \bar{g}}{\partial x} \right) \delta y dx \\ &= (g, \delta y) \end{aligned}$$

where

$$\bar{g} - \frac{\partial}{\partial x} \epsilon \frac{\partial \bar{g}}{\partial x} = g$$

and  $\bar{g} = 0$  at the end points. Thus  $\bar{g}$  can be obtained from  $g$  by a smoothing equation. Now the step

$$y^{n+1} = y^n - \lambda^n \bar{g}^n$$

gives an improvement

$$\delta I = -\lambda^n \langle \bar{g}^n, \bar{g}^n \rangle$$

but  $y^{n+1}$  has the same smoothness as  $y^n$ , resulting in a stable process.

## 5.2 Sobolev gradient for shape optimization

In applying control theory to aerodynamic shape optimization, the use of a Sobolev gradient is equally important for the preservation of the smoothness class of the redesigned surface. Accordingly, using the weighted Sobolev inner product defined above, we define a modified gradient  $\bar{\mathcal{G}}$  such that

$$\delta I = \langle \bar{\mathcal{G}}, \delta \mathcal{F} \rangle.$$

In the one dimensional case  $\bar{\mathcal{G}}$  is obtained by solving the smoothing equation

$$\bar{\mathcal{G}} - \frac{\partial}{\partial \xi_1} \epsilon \frac{\partial \bar{\mathcal{G}}}{\partial \xi_1} = \mathcal{G}. \quad (37)$$

In the multi-dimensional case the smoothing is applied in product form. Finally we set

$$\delta \mathcal{F} = -\lambda \bar{\mathcal{G}} \quad (38)$$

with the result that

$$\delta I = -\lambda \langle \bar{\mathcal{G}}, \bar{\mathcal{G}} \rangle < 0,$$

unless  $\bar{\mathcal{G}} = 0$ , and correspondingly  $\mathcal{G} = 0$ .

When second-order central differencing is applied to (37), the equation at a given node,  $i$ , can be expressed as

$$\bar{\mathcal{G}}_i - \epsilon (\bar{\mathcal{G}}_{i+1} - 2\bar{\mathcal{G}}_i + \bar{\mathcal{G}}_{i-1}) = \mathcal{G}_i, \quad 1 \leq i \leq n,$$

where  $\mathcal{G}_i$  and  $\bar{\mathcal{G}}_i$  are the point gradients at node  $i$  before and after the smoothing respectively, and  $n$  is the number of design variables equal to the number of mesh points in this case. Then,

$$\bar{\mathcal{G}} = A\mathcal{G},$$

where  $A$  is the  $n \times n$  tri-diagonal matrix such that

$$A^{-1} = \begin{bmatrix} 1 + 2\epsilon - \epsilon & 0 & & & 0 \\ \epsilon & \cdot & \cdot & & \\ 0 & \cdot & \cdot & \cdot & \\ \cdot & & \cdot & \cdot & -\epsilon \\ 0 & & \epsilon & 1 + 2\epsilon & \end{bmatrix}.$$

Using the steepest descent method in each design iteration, a step,  $\delta \mathcal{F}$ , is taken such that

$$\delta \mathcal{F} = -\lambda A\mathcal{G}. \quad (39)$$

As can be seen from the form of this expression, implicit smoothing may be regarded as a preconditioner which allows the use of much larger steps for the search procedure and leads to a large reduction in the number of design iterations needed for convergence. Our software also includes an option for Krylov acceleration [25]. We have found this to be particularly useful for inverse problems.

### 5.3 Outline of the design procedure

The design procedure can finally be summarized as follows:

1. Solve the flow equations for  $\rho$ ,  $u_1$ ,  $u_2$ ,  $u_3$ ,  $p$ .
2. Solve the adjoint equations for  $\psi$  subject to appropriate boundary conditions.
3. Evaluate  $\mathcal{G}$  and calculate the corresponding Sobolev gradient  $\bar{\mathcal{G}}$ .
4. Project  $\bar{\mathcal{G}}$  into an allowable subspace that satisfies any geometric constraints.
5. Update the shape based on the direction of steepest descent.
6. Return to 1 until convergence is reached.

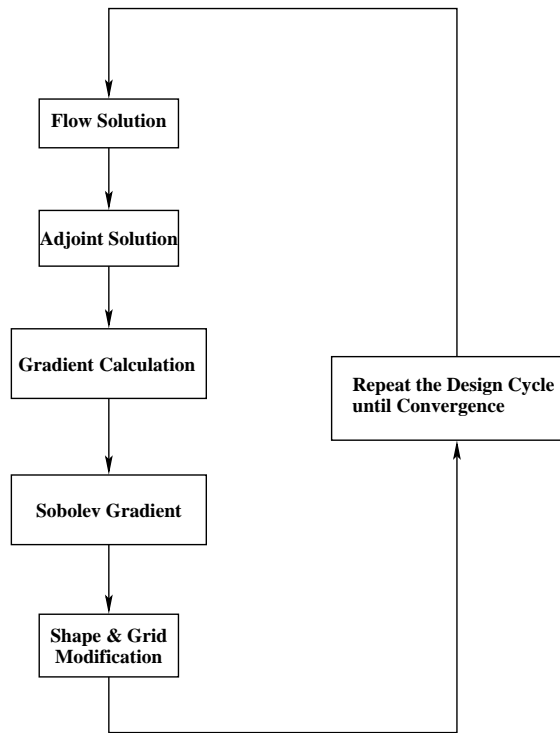


Fig. 1. Design cycle

Practical implementation of the design method relies heavily upon fast and accurate solvers for both the state ( $w$ ) and co-state ( $\psi$ ) systems. The result obtained in Section 8 have been obtained using well-validated software for the solution of the Euler and Navier-Stokes equations developed over the course of many years [26–28]. For inverse design the lift is fixed by the target pressure. In drag minimization it is also appropriate to fix the lift coefficient, because the induced drag is a major fraction of the total drag, and this could be reduced simply by reducing the lift. Therefore the angle of attack is adjusted during each flow solution to force a specified lift coefficient to be attained, and the influence of variations of the angle of attack is included in the calculation of the gradient. The vortex drag also depends on the span loading, which may be constrained by other considerations such as structural loading or buffet onset. Consequently, the option is provided to force the span loading by adjusting the twist distribution as well as the angle of attack during the flow solution.

## 6 Design using the Navier-Stokes Equations

### 6.1 The Navier-Stokes equations in the computational domain

The next sections present the extension of the adjoint method to the Navier-Stokes equations. These take the form

$$\frac{\partial w}{\partial t} + \frac{\partial f_i}{\partial x_i} = \frac{\partial f_{vi}}{\partial x_i} \quad \text{in } \mathcal{D}, \quad (40)$$

where the state vector  $w$ , inviscid flux vector  $f$  and viscous flux vector  $f_v$  are described respectively by

$$w = \begin{pmatrix} \rho \\ \rho u_1 \\ \rho u_2 \\ \rho u_3 \\ \rho E \end{pmatrix}, \quad f_i = \begin{pmatrix} \rho u_i \\ \rho u_i u_1 + p \delta_{i1} \\ \rho u_i u_2 + p \delta_{i2} \\ \rho u_i u_3 + p \delta_{i3} \\ \rho u_i H \end{pmatrix}, \quad f_{vi} = \begin{pmatrix} 0 \\ \sigma_{ij} \delta_{j1} \\ \sigma_{ij} \delta_{j2} \\ \sigma_{ij} \delta_{j3} \\ u_j \sigma_{ij} + k \frac{\partial T}{\partial x_i} \end{pmatrix}. \quad (41)$$

The viscous stresses may be written as

$$\sigma_{ij} = \mu \left( \frac{\partial u_i}{\partial x_j} + \frac{\partial u_j}{\partial x_i} \right) + \lambda \delta_{ij} \frac{\partial u_k}{\partial x_k}, \quad (42)$$

where  $\mu$  and  $\lambda$  are the first and second coefficients of viscosity. The coefficient of thermal conductivity and the temperature are computed as

$$k = \frac{c_p \mu}{Pr}, \quad T = \frac{p}{R\rho}, \quad (43)$$

where  $Pr$  is the Prandtl number,  $c_p$  is the specific heat at constant pressure, and  $R$  is the gas constant.

Using a transformation to a fixed computational domain as before, the Navier-Stokes equations can be written in the transformed coordinates as

$$\frac{\partial (Jw)}{\partial t} + \frac{\partial (F_i - F_{vi})}{\partial \xi_i} = 0 \quad \text{in } \mathcal{D}, \quad (44)$$

where the viscous terms have the form

$$\frac{\partial F_{vi}}{\partial \xi_i} = \frac{\partial}{\partial \xi_i} (S_{ij} f_{vj}).$$

Computing the variation  $\delta w$  resulting from a shape modification of the boundary, introducing a co-state vector  $\psi$  and integrating by parts, following the steps outlined by equations (19) to (22), we obtain

$$\int_{\mathcal{B}} \psi^T (\delta S_{2j} f_{vj} + S_{2j} \delta f_{vj}) d\mathcal{B}_\xi - \int_{\mathcal{D}} \frac{\partial \psi^T}{\partial \xi_i} (\delta S_{ij} f_{vj} + S_{ij} \delta f_{vj}) d\mathcal{D}_\xi,$$

where the shape modification is restricted to the coordinate surface  $\xi_2 = 0$  so that  $n_1 = n_3 = 0$ , and  $n_2 = 1$ . Furthermore, it is assumed that the boundary contributions at the far field may either be neglected or else eliminated by a proper choice of boundary conditions as previously shown for the inviscid case [14,29].

The viscous terms will be derived under the assumption that the viscosity and heat conduction coefficients  $\mu$  and  $k$  are essentially independent of the flow, and that their variations may be neglected. This simplification has been successfully used for many aerodynamic problems of interest. However, if the flow variations could result in significant changes in the turbulent viscosity, it may be necessary to account for its variation in the calculation.

### 6.2 Transformation to Primitive Variables

The derivation of the viscous adjoint terms can be simplified by transforming to the primitive variables

$$\tilde{w}^T = (\rho, u_1, u_2, u_3, p)^T,$$

because the viscous stresses depend on the velocity derivatives  $\frac{\partial u_i}{\partial x_j}$ , while the heat flux can be expressed as

$$\kappa \frac{\partial}{\partial x_i} \left( \frac{p}{\rho} \right).$$

where  $\kappa = \frac{k}{R} = \frac{\gamma \mu}{Pr(\gamma-1)}$ . The relationship between the conservative and primitive variations is defined by the expressions

$$\delta w = M \delta \tilde{w}, \quad \delta \tilde{w} = M^{-1} \delta w$$

which make use of the transformation matrices  $M = \frac{\partial w}{\partial \tilde{w}}$  and  $M^{-1} = \frac{\partial \tilde{w}}{\partial w}$ . These matrices are provided in transposed form for future convenience

$$M^T = \begin{bmatrix} 1 & u_1 & u_2 & u_3 & \frac{u_i u_i}{2} \\ 0 & \rho & 0 & 0 & \rho u_1 \\ 0 & 0 & \rho & 0 & \rho u_2 \\ 0 & 0 & 0 & \rho & \rho u_3 \\ 0 & 0 & 0 & 0 & \frac{1}{\gamma-1} \end{bmatrix}$$

$$M^{-1T} = \begin{bmatrix} 1 & -\frac{u_1}{\rho} & -\frac{u_2}{\rho} & -\frac{u_3}{\rho} & \frac{(\gamma-1)u_i u_i}{2} \\ 0 & \frac{1}{\rho} & 0 & 0 & -(\gamma-1)u_1 \\ 0 & 0 & \frac{1}{\rho} & 0 & -(\gamma-1)u_2 \\ 0 & 0 & 0 & \frac{1}{\rho} & -(\gamma-1)u_3 \\ 0 & 0 & 0 & 0 & \gamma-1 \end{bmatrix}.$$

The conservative and primitive adjoint operators  $L$  and  $\tilde{L}$  corresponding to the variations  $\delta w$  and  $\delta \tilde{w}$  are then related by

$$\int_{\mathcal{D}} \delta w^T L \psi \, d\mathcal{D}_\xi = \int_{\mathcal{D}} \delta \tilde{w}^T \tilde{L} \psi \, d\mathcal{D}_\xi,$$

with

$$\tilde{L} = M^T L,$$

so that after determining the primitive adjoint operator by direct evaluation of the viscous portion of (24), the conservative operator may be obtained by the transformation  $L = M^{-1T} \tilde{L}$ . Since the continuity equation contains no viscous terms, it makes no contribution to the viscous adjoint system. Therefore, the derivation proceeds by first examining the adjoint operators arising from the momentum equations.

### 6.3 Contributions from the Momentum Equations

In order to make use of the summation convention, it is convenient to set  $\psi_{j+1} = \phi_j$  for  $j = 1, 2, 3$ . Then the contribution from the momentum equations is

$$\int_{\mathcal{B}} \phi_k (\delta S_{2j} \sigma_{kj} + S_{2j} \delta \sigma_{kj}) \, d\mathcal{B}_\xi - \int_{\mathcal{D}} \frac{\partial \phi_k}{\partial \xi_i} (\delta S_{ij} \sigma_{kj} + S_{ij} \delta \sigma_{kj}) \, d\mathcal{D}_\xi. \quad (45)$$

The velocity derivatives can be expressed as

$$\frac{\partial u_i}{\partial x_j} = \frac{\partial u_i}{\partial \xi_l} \frac{\partial \xi_l}{\partial x_j} = \frac{S_{lj}}{J} \frac{\partial u_i}{\partial \xi_l}$$

with corresponding variations

$$\delta \frac{\partial u_i}{\partial x_j} = \left[ \frac{S_{lj}}{J} \right]_I \frac{\partial}{\partial \xi_l} \delta u_i + \left[ \frac{\partial u_i}{\partial \xi_l} \right]_{II} \delta \left( \frac{S_{lj}}{J} \right).$$

The variations in the stresses are then

$$\begin{aligned} \delta \sigma_{kj} = & \left\{ \mu \left[ \frac{S_{lj}}{J} \frac{\partial}{\partial \xi_l} \delta u_k + \frac{S_{lk}}{J} \frac{\partial}{\partial \xi_l} \delta u_j \right] + \lambda \left[ \delta_{jk} \frac{S_{lm}}{J} \frac{\partial}{\partial \xi_l} \delta u_m \right] \right\}_I \\ & + \left\{ \mu \left[ \delta \left( \frac{S_{lj}}{J} \right) \frac{\partial u_k}{\partial \xi_l} + \delta \left( \frac{S_{lk}}{J} \right) \frac{\partial u_j}{\partial \xi_l} \right] + \lambda \left[ \delta_{jk} \delta \left( \frac{S_{lm}}{J} \right) \frac{\partial u_m}{\partial \xi_l} \right] \right\}_{II}. \end{aligned}$$

As before, only those terms with subscript  $I$ , which contain variations of the flow variables, need be considered further in deriving the adjoint operator. The field contributions that contain  $\delta u_i$  in equation (45) appear as

$$- \int_{\mathcal{D}} \frac{\partial \phi_k}{\partial \xi_i} S_{ij} \left\{ \mu \left( \frac{S_{lj}}{J} \frac{\partial}{\partial \xi_l} \delta u_k + \frac{S_{lk}}{J} \frac{\partial}{\partial \xi_l} \delta u_j \right) + \lambda \delta_{jk} \frac{S_{lm}}{J} \frac{\partial}{\partial \xi_l} \delta u_m \right\} d\mathcal{D}_\xi.$$

This may be integrated by parts to yield

$$\begin{aligned} & \int_{\mathcal{D}} \delta u_k \frac{\partial}{\partial \xi_l} \left( S_{lj} S_{ij} \frac{\mu}{J} \frac{\partial \phi_k}{\partial \xi_i} \right) d\mathcal{D}_\xi \\ & + \int_{\mathcal{D}} \delta u_j \frac{\partial}{\partial \xi_l} \left( S_{lk} S_{ij} \frac{\mu}{J} \frac{\partial \phi_k}{\partial \xi_i} \right) d\mathcal{D}_\xi \\ & + \int_{\mathcal{D}} \delta u_m \frac{\partial}{\partial \xi_l} \left( S_{lm} S_{ij} \frac{\lambda \delta_{jk}}{J} \frac{\partial \phi_k}{\partial \xi_i} \right) d\mathcal{D}_\xi, \end{aligned}$$

where the boundary integral has been eliminated by noting that  $\delta u_i = 0$  on the solid boundary. By exchanging indices, the field integrals may be combined to produce

$$\int_{\mathcal{D}} \delta u_k \frac{\partial}{\partial \xi_l} S_{lj} \left\{ \mu \left( \frac{S_{ij}}{J} \frac{\partial \phi_k}{\partial \xi_i} + \frac{S_{ik}}{J} \frac{\partial \phi_j}{\partial \xi_i} \right) + \lambda \delta_{jk} \frac{S_{im}}{J} \frac{\partial \phi_m}{\partial \xi_i} \right\} d\mathcal{D}_\xi,$$

which is further simplified by transforming the inner derivatives back to Cartesian coordinates

$$\int_{\mathcal{D}} \delta u_k \frac{\partial}{\partial \xi_l} S_{lj} \left\{ \mu \left( \frac{\partial \phi_k}{\partial x_j} + \frac{\partial \phi_j}{\partial x_k} \right) + \lambda \delta_{jk} \frac{\partial \phi_m}{\partial x_m} \right\} d\mathcal{D}_\xi. \quad (46)$$

The boundary contributions that contain  $\delta u_i$  in equation (45) may be simplified using the fact that

$$\frac{\partial}{\partial \xi_l} \delta u_i = 0 \quad \text{if } l = 1, 3$$

on the boundary  $\mathcal{B}$  so that they become

$$\int_{\mathcal{B}} \phi_k S_{2j} \left\{ \mu \left( \frac{S_{2j}}{J} \frac{\partial}{\partial \xi_2} \delta u_k + \frac{S_{2k}}{J} \frac{\partial}{\partial \xi_2} \delta u_j \right) + \lambda \delta_{jk} \frac{S_{2m}}{J} \frac{\partial}{\partial \xi_2} \delta u_m \right\} d\mathcal{B}_\xi. \quad (47)$$

Together, (46) and (47) comprise the field and boundary contributions of the momentum equations to the viscous adjoint operator in primitive variables.

#### 6.4 Contributions from the Energy Equation

In order to derive the contribution of the energy equation to the viscous adjoint terms it is convenient to set

$$\psi_5 = \theta, \quad Q_j = u_i \sigma_{ij} + \kappa \frac{\partial}{\partial x_j} \left( \frac{p}{\rho} \right),$$

where the temperature has been written in terms of pressure and density using (43). The contribution from the energy equation can then be written as

$$\int_{\mathcal{B}} \theta (\delta S_{2j} Q_j + S_{2j} \delta Q_j) d\mathcal{B}_\xi - \int_{\mathcal{D}} \frac{\partial \theta}{\partial \xi_i} (\delta S_{ij} Q_j + S_{ij} \delta Q_j) d\mathcal{D}_\xi. \quad (48)$$

The field contributions that contain  $\delta u_i, \delta p$ , and  $\delta \rho$  in equation (48) appear as

$$- \int_{\mathcal{D}} \frac{\partial \theta}{\partial \xi_i} S_{ij} \delta Q_j d\mathcal{D}_\xi = - \int_{\mathcal{D}} \frac{\partial \theta}{\partial \xi_i} S_{ij} \left\{ \delta u_k \sigma_{kj} + u_k \delta \sigma_{kj} + \kappa \frac{S_{lj}}{J} \frac{\partial}{\partial \xi_l} \left( \frac{\delta p}{\rho} - \frac{p}{\rho} \frac{\delta \rho}{\rho} \right) \right\} d\mathcal{D}_\xi. \quad (49)$$

The term involving  $\delta\sigma_{kj}$  may be integrated by parts to produce

$$\int_{\mathcal{D}} \delta u_k \frac{\partial}{\partial \xi_l} S_{lj} \left\{ \mu \left( u_k \frac{\partial \theta}{\partial x_j} + u_j \frac{\partial \theta}{\partial x_k} \right) + \lambda \delta_{jk} u_m \frac{\partial \theta}{\partial x_m} \right\} d\mathcal{D}_\xi, \quad (50)$$

where the conditions  $u_i = \delta u_i = 0$  are used to eliminate the boundary integral on  $\mathcal{B}$ . Notice that the other term in (49) that involves  $\delta u_k$  need not be integrated by parts and is merely carried on as

$$- \int_{\mathcal{D}} \delta u_k \sigma_{kj} S_{ij} \frac{\partial \theta}{\partial \xi_i} d\mathcal{D}_\xi \quad (51)$$

The terms in expression (49) that involve  $\delta p$  and  $\delta \rho$  may also be integrated by parts to produce both a field and a boundary integral. The field integral becomes

$$\int_{\mathcal{D}} \left( \frac{\delta p}{\rho} - \frac{p \delta \rho}{\rho^2} \right) \frac{\partial}{\partial \xi_l} \left( S_{lj} S_{ij} \frac{\kappa}{J} \frac{\partial \theta}{\partial \xi_i} \right) d\mathcal{D}_\xi$$

which may be simplified by transforming the inner derivative to Cartesian coordinates

$$\int_{\mathcal{D}} \left( \frac{\delta p}{\rho} - \frac{p \delta \rho}{\rho^2} \right) \frac{\partial}{\partial \xi_i} \left( S_{lj} \kappa \frac{\partial \theta}{\partial x_j} \right) d\mathcal{D}_\xi. \quad (52)$$

The boundary integral becomes

$$\int_{\mathcal{B}} \kappa \left( \frac{\delta p}{\rho} - \frac{p \delta \rho}{\rho^2} \right) \frac{S_{2j} S_{ij}}{J} \frac{\partial \theta}{\partial \xi_i} d\mathcal{B}_\xi. \quad (53)$$

This can be simplified by transforming the inner derivative to Cartesian coordinates

$$\int_{\mathcal{B}} \kappa \left( \frac{\delta p}{\rho} - \frac{p \delta \rho}{\rho^2} \right) \frac{S_{2j}}{J} \frac{\partial \theta}{\partial x_j} d\mathcal{B}_\xi, \quad (54)$$

and identifying the normal derivative at the wall

$$\frac{\partial}{\partial n} = S_{2j} \frac{\partial}{\partial x_j}, \quad (55)$$

and the variation in temperature

$$\delta T = \frac{1}{R} \left( \frac{\delta p}{\rho} - \frac{p \delta \rho}{\rho^2} \right),$$

to produce the boundary contribution

$$\int_{\mathcal{B}} k \delta T \frac{\partial \theta}{\partial n} d\mathcal{B}_\xi. \quad (56)$$

This term vanishes if  $T$  is constant on the wall but persists if the wall is adiabatic.

There is also a boundary contribution left over from the first integration by parts (48) which has the form

$$\int_{\mathcal{B}} \theta \delta (S_{2j} Q_j) d\mathcal{B}_\xi, \quad (57)$$

where

$$Q_j = k \frac{\partial T}{\partial x_j},$$

since  $u_i = 0$ . If the wall is adiabatic

$$\frac{\partial T}{\partial n} = 0,$$

so that using (55),

$$\delta (S_{2j} Q_j) = 0,$$

and both the  $\delta w$  and  $\delta S$  boundary contributions vanish.

On the other hand, if  $T$  is constant  $\frac{\partial T}{\partial \xi_l} = 0$  for  $l = 1, 3$ , so that

$$Q_j = k \frac{\partial T}{\partial x_j} = k \left( \frac{S_{lj}}{J} \frac{\partial T}{\partial \xi_l} \right) = k \left( \frac{S_{2j}}{J} \frac{\partial T}{\partial \xi_2} \right).$$

Thus, the boundary integral (57) becomes

$$\int_{\mathcal{B}} k\theta \left\{ \frac{S_{2j}^2}{J} \frac{\partial}{\partial \xi_2} \delta T + \delta \left( \frac{S_{2j}^2}{J} \right) \frac{\partial T}{\partial \xi_2} \right\} d\mathcal{B}_\xi. \quad (58)$$

Therefore, for constant  $T$ , the first term corresponding to variations in the flow field contributes to the adjoint boundary operator, and the second set of terms corresponding to metric variations contribute to the cost function gradient.

Finally the contributions from the energy equation to the viscous adjoint operator are the three field terms (50), (51) and (52), and either of two boundary contributions (56) or (58), depending on whether the wall is adiabatic or has constant temperature.

## 6.5 The Viscous Adjoint Field Operator

Collecting together the contributions from the momentum and energy equations, the viscous adjoint operator in primitive variables can be expressed as

$$\begin{aligned} (\tilde{L}\psi)_1 &= -\frac{p}{\rho^2} \frac{\partial}{\partial \xi_l} \left( S_{lj} \kappa \frac{\partial \theta}{\partial x_j} \right) \\ (\tilde{L}\psi)_{i+1} &= \frac{\partial}{\partial \xi_l} \left\{ S_{lj} \left[ \mu \left( \frac{\partial \phi_i}{\partial x_j} + \frac{\partial \phi_j}{\partial x_i} \right) + \lambda \delta_{ij} \frac{\partial \phi_k}{\partial x_k} \right] \right\} \\ &\quad + \frac{\partial}{\partial \xi_l} \left\{ S_{lj} \left[ \mu \left( u_i \frac{\partial \theta}{\partial x_j} + u_j \frac{\partial \theta}{\partial x_i} \right) + \lambda \delta_{ij} u_k \frac{\partial \theta}{\partial x_k} \right] \right\} \quad \text{for } i = 1, 2, 3 \\ &\quad - \sigma_{ij} S_{lj} \frac{\partial \theta}{\partial \xi_l} \\ (\tilde{L}\psi)_5 &= \frac{1}{\rho} \frac{\partial}{\partial \xi_l} \left( S_{lj} \kappa \frac{\partial \theta}{\partial x_j} \right). \end{aligned}$$

The conservative viscous adjoint operator may now be obtained by the transformation

$$L = M^{-1T} \tilde{L}.$$

## 7 Viscous Adjoint Boundary Conditions

It was recognized in Section 3 that the boundary conditions satisfied by the flow equations restrict the form of the performance measure that may be chosen for the cost function. There must be a direct correspondence between the flow variables for which variations appear in the variation of the cost function, and those variables for which variations appear in the boundary terms arising during the derivation of the adjoint field equations. Otherwise it would be impossible to eliminate the dependence of  $\delta I$  on  $\delta w$  through proper specification of the adjoint boundary condition. Consequently the contributions of the pressure and viscous stresses need to be merged. As in the derivation of the field equations, it proves convenient to consider the contributions from the momentum equations and the energy equation separately.

### 7.1 Boundary Conditions Arising from the Momentum Equations

The boundary term that arises from the momentum equations including both the  $\delta w$  and  $\delta S$  components (45) takes the form

$$\int_{\mathcal{B}} \phi_k \delta (S_{2j} (\delta_{kj} p + \sigma_{kj})) d\mathcal{B}_\xi.$$

Replacing the metric term with the corresponding local face area  $S_2$  and unit normal  $n_j$  defined by

$$|S_2| = \sqrt{S_{2j}S_{2j}}, \quad n_j = \frac{S_{2j}}{|S_2|}$$

then leads to

$$\int_{\mathcal{B}} \phi_k \delta (|S_2| n_j (\delta_{kj} p + \sigma_{kj})) d\mathcal{B}_\xi.$$

Defining the components of the total surface stress as

$$\tau_k = n_j (\delta_{kj} p + \sigma_{kj})$$

and the physical surface element

$$dS = |S_2| d\mathcal{B}_\xi,$$

the integral may then be split into two components

$$\int_{\mathcal{B}} \phi_k \tau_k |\delta S_2| d\mathcal{B}_\xi + \int_{\mathcal{B}} \phi_k \delta \tau_k dS, \quad (59)$$

where only the second term contains variations in the flow variables and must consequently cancel the  $\delta w$  terms arising in the cost function. The first term will appear in the expression for the gradient.

A general expression for the cost function that allows cancellation with terms containing  $\delta \tau_k$  has the form

$$I = \int_{\mathcal{B}} \mathcal{N}(\tau) dS, \quad (60)$$

corresponding to a variation

$$\delta I = \int_{\mathcal{B}} \frac{\partial \mathcal{N}}{\partial \tau_k} \delta \tau_k dS,$$

for which cancellation is achieved by the adjoint boundary condition

$$\phi_k = \frac{\partial \mathcal{N}}{\partial \tau_k}.$$

Natural choices for  $\mathcal{N}$  arise from force optimization and as measures of the deviation of the surface stresses from desired target values.

The force in a direction with cosines  $q_i$  has the form

$$C_q = \int_{\mathcal{B}} q_i \tau_i dS.$$

If we take this as the cost function (60), this quantity gives

$$\mathcal{N} = q_i \tau_i.$$

Cancellation with the flow variation terms in equation (59) therefore mandates the adjoint boundary condition

$$\phi_k = q_k.$$

Note that this choice of boundary condition also eliminates the first term in equation (59) so that it need not be included in the gradient calculation.

In the inverse design case, where the cost function is intended to measure the deviation of the surface stresses from some desired target values, a suitable definition is

$$\mathcal{N}(\tau) = \frac{1}{2} a_{lk} (\tau_l - \tau_{dl}) (\tau_k - \tau_{dk}),$$

where  $\tau_d$  is the desired surface stress, including the contribution of the pressure, and the coefficients  $a_{lk}$  define a weighting matrix. For cancellation

$$\phi_k \delta \tau_k = a_{lk} (\tau_l - \tau_{dl}) \delta \tau_k.$$

This is satisfied by the boundary condition

$$\phi_k = a_{lk} (\tau_l - \tau_d). \quad (61)$$

Assuming arbitrary variations in  $\delta\tau_k$ , this condition is also necessary.

In order to control the surface pressure and normal stress one can measure the difference

$$n_j \{ \sigma_{kj} + \delta_{kj} (p - p_d) \},$$

where  $p_d$  is the desired pressure. The normal component is then

$$\tau_n = n_k n_j \sigma_{kj} + p - p_d,$$

so that the measure becomes

$$\begin{aligned} \mathcal{N}(\tau) &= \frac{1}{2} \tau_n^2 \\ &= \frac{1}{2} n_l n_m n_k n_j \{ \sigma_{lm} + \delta_{lm} (p - p_d) \} \{ \sigma_{kj} + \delta_{kj} (p - p_d) \}. \end{aligned}$$

This corresponds to setting

$$a_{lk} = n_l n_k$$

in equation (61). Defining the viscous normal stress as

$$\tau_{vn} = n_k n_j \sigma_{kj},$$

the measure can be expanded as

$$\begin{aligned} \mathcal{N}(\tau) &= \frac{1}{2} n_l n_m n_k n_j \sigma_{lm} \sigma_{kj} + \frac{1}{2} (n_k n_j \sigma_{kj} + n_l n_m \sigma_{lm}) (p - p_d) + \frac{1}{2} (p - p_d)^2 \\ &= \frac{1}{2} \tau_{vn}^2 + \tau_{vn} (p - p_d) + \frac{1}{2} (p - p_d)^2. \end{aligned}$$

For cancellation of the boundary terms

$$\phi_k (n_j \delta \sigma_{kj} + n_k \delta p) = \{ n_l n_m \sigma_{lm} + n_l^2 (p - p_d) \} n_k (n_j \delta \sigma_{kj} + n_k \delta p)$$

leading to the boundary condition

$$\phi_k = n_k (\tau_{vn} + p - p_d).$$

In the case of high Reynolds number, this is well approximated by the equations

$$\phi_k = n_k (p - p_d), \quad (62)$$

which should be compared with the single scalar equation derived for the inviscid boundary condition (29). In the case of an inviscid flow, choosing

$$\mathcal{N}(\tau) = \frac{1}{2} (p - p_d)^2$$

requires

$$\phi_k n_k \delta p = (p - p_d) n_k^2 \delta p = (p - p_d) \delta p$$

which is satisfied by equation (62), but which represents an overspecification of the boundary condition since only the single condition (29) needs be specified to ensure cancellation.

## Boundary Conditions Arising from the Energy Equation

The form of the boundary terms arising from the energy equation depends on the choice of temperature boundary condition at the wall. For the adiabatic case, the boundary contribution is (56)

$$\int_{\mathcal{B}} k\delta T \frac{\partial\theta}{\partial n} d\mathcal{B}_{\xi},$$

while for the constant temperature case the boundary term is (58). One possibility is to introduce a contribution into the cost function which depends on  $T$  or  $\frac{\partial T}{\partial n}$  so that the appropriate cancellation would occur. Since there is little physical intuition to guide the choice of such a cost function for aerodynamic design, a more natural solution is to set

$$\theta = 0$$

in the constant temperature case or

$$\frac{\partial\theta}{\partial n} = 0$$

in the adiabatic case. Note that in the constant temperature case, this choice of  $\theta$  on the boundary would also eliminate the boundary metric variation terms in (57).

## 8 Results

### 8.1 Redesign of the Boeing 747 wing

Over the last decade the adjoint method has been successfully used to refine a variety of designs for flight at both transonic and supersonic cruising speeds. In the case of transonic flight, it is often possible to produce a shock free flow which eliminates the shock drag by making very small changes, typically no larger than the boundary layer displacement thickness. Consequently viscous effects need to be considered in order to realize the full benefits of the optimization.

Here the optimization of the wing of the Boeing 747-200 is presented to illustrate the kind of benefits that can be obtained. In these calculations the flow was modeled by the Reynolds Averaged Navier-Stokes equations. A Baldwin Lomax turbulence model was considered sufficient, since the optimization is for the cruise condition with attached flow. The calculation were performed to minimize the drag coefficient at a fixed lift coefficient, subject to the additional constraints that the span loading should not be altered and the thickness should not be reduced. It might be possible to reduce the induced drag by modifying the span loading to an elliptic distribution, but this would increase the root bending moment, and consequently require an increase in the skin thickness and structure weight. A reduction in wing thickness would not only reduce the fuel volume, but it would also require an increase in skin thickness to support the bending moment. Thus these constraints assure that there will be no penalty in either structure weight or fuel volume.

Figure 2 displays the result of an optimization at a Mach number of 0.86, which is roughly the maximum cruising Mach number attainable by the existing design before the onset of significant drag rise. The lift coefficient of 0.42 is the contribution of the exposed wing. Allowing for the fuselage to total lift coefficient is about 0.47. It can be seen that the redesigned wing is essentially shock free, and the drag coefficient is reduced from 0.01269 (127 counts) to 0.01136 (114 counts). The total drag coefficient of the aircraft at this lift coefficient is around 270 counts, so this would represent a drag reduction of the order of 5 percent.

Figure 3 displays the result of an optimization at Mach 0.90. In this case the shock waves are not eliminated, but their strength is significantly weakened, while the drag coefficient is reduced from 0.01819 (182 counts) to 0.01293 (129 counts). Thus the redesigned wing has essentially the same drag at Mach 0.9 as the original wing at Mach 0.86. The Boeing 747 wing could apparently be modified to allow such an increase in the cruising Mach number because it has a higher sweep-back than later designs, and a rather thin wing section with a thickness to chord ratio of 8 percent. Figures 4 and 5 verify that the span loading and thickness were not changed by the redesign, while figures 6 and 7 indicate the required section changes at 42 percent and 68 percent span stations.

## 8.2 Wing design using an unstructured mesh

A major obstacle to the treatment of arbitrarily complex configurations is the difficulty and cost of mesh generation. This can be mitigated by the use of unstructured meshes. Thus it appears that the extension of the adjoint method to unstructured meshes may provide the most promising route to the optimum shape design of key elements of complex configurations, such as wing-pylon-nacelle combinations. Some preliminary results are presented below. These have been obtained with new software to implement the adjoint method for unstructured meshes which is currently under development [30]. Figures 8 and 9 shows the result of an inverse design calculation, where the initial geometry was a wing made up of NACA 0012 sections and the target pressure distribution was the pressure distribution over the Onera M6 wing. Figures 10, 11, 12, 13, 14, 15, show the target and computed pressure distribution at six span-wise sections. It can be seen from these plots the target pressure distribution is well recovered in 50 design cycles, verifying that the design process is capable of recovering pressure distributions that are significantly different from the initial distribution. This is a particularly challenging test, because it calls for the recovery of a smooth symmetric profile from an asymmetric pressure distribution containing a triangular pattern of shock waves.

Another test case for the inverse design problem uses the wing from an airplane (code named SHARK) [31] which has been designed for the Reno Air Races. The initial and final pressure distributions are shown the figure 16. As can be seen from these plots, the initial pressure distribution has a weak shock in the outboard sections of the wing, while the final pressure distribution is shock-free. The final pressure distributions are compared with the target distributions along three sections of the wing in figures 17, 18, 19. Again the design process captures the target pressure with good accuracy in about 50 design cycles. The drag minimization problem has also been studied for this wing, and the results are shown in figure 20. As can be seen from this plot, the final geometry has a shock-free profile and the drag coefficient has been slightly reduced.

## 9 Conclusion

The accumulated experience of the last decade suggests that most existing aircraft which cruise at transonic speeds are amenable to a drag reduction of the order of 3 to 5 percent, or an increase in the drag rise Mach number of at least .02. These improvements can be achieved by very small shape modifications, which are too subtle to allow their determination by trial and error methods. The potential economic benefits are substantial, considering the fuel costs of the entire airline fleet. Moreover, if one were to take full advantage of the increase in the lift to drag ratio during the design process, a smaller aircraft could be designed to perform the same task, with consequent further cost reductions. It seems inevitable that some method of this type will provide a basis for aerodynamic designs of the future.

## Acknowledgment

This work has benefited greatly from the support of the Air Force Office of Science Research under grant No. AF F49620-98-1-2002. I have drawn extensively from the lecture notes prepared by Luigi Martinelli and myself for a CIME summer course in 1999 [32]. I am also indebted to my research assistant Kasidit Leoviriyakit for his assistance in preparing the Latex files for this text.

## References

1. R. M. Hicks, E. M. Murman, and G. N. Vanderplaats. An assessment of airfoil design by numerical optimization. *NASA TM X-3092*, Ames Research Center, Moffett Field, California, July 1974.
2. R. M. Hicks and P. A. Henne. Wing design by numerical optimization. *Journal of Aircraft*, 15:407–412, 1978.
3. J. L. Lions. *Optimal Control of Systems Governed by Partial Differential Equations*. Springer-Verlag, New York, 1971. Translated by S.K. Mitter.
4. A. E. Bryson and Y. C. Ho. *Applied Optimal Control*. Hemisphere, Washington, DC, 1975.
5. M. J. Lighthill. A new method of two-dimensional aerodynamic design. *R & M 1111*, Aeronautical Research Council, 1945.
6. O. Pironneau. *Optimal Shape Design for Elliptic Systems*. Springer-Verlag, New York, 1984.

7. A. Jameson. Optimum aerodynamic design using CFD and control theory. *AIAA paper 95-1729*, AIAA 12th Computational Fluid Dynamics Conference, San Diego, CA, June 1995.
8. A. Jameson. Aerodynamic design via control theory. *Journal of Scientific Computing*, 3:233–260, 1988.
9. A. Jameson and J.J. Alonso. Automatic aerodynamic optimization on distributed memory architectures. *AIAA paper 96-0409*, 34th Aerospace Sciences Meeting and Exhibit, Reno, Nevada, January 1996.
10. A. Jameson. Re-engineering the design process through computation. *AIAA paper 97-0641*, 35th Aerospace Sciences Meeting and Exhibit, Reno, Nevada, January 1997.
11. A. Jameson, N. Pierce, and L. Martinelli. Optimum aerodynamic design using the Navier-Stokes equations. *AIAA paper 97-0101*, 35th Aerospace Sciences Meeting and Exhibit, Reno, Nevada, January 1997.
12. A. Jameson, L. Martinelli, and N. A. Pierce. Optimum aerodynamic design using the Navier-Stokes equations. *Theoret. Comput. Fluid Dynamics*, 10:213–237, 1998.
13. A. Jameson. Computational aerodynamics for aircraft design. *Science*, 245:361–371, July 1989.
14. A. Jameson. Automatic design of transonic airfoils to reduce the shock induced pressure drag. In *Proceedings of the 31st Israel Annual Conference on Aviation and Aeronautics, Tel Aviv*, pages 5–17, February 1990.
15. A. Jameson. Optimum aerodynamic design via boundary control. In *AGARD-VKI Lecture Series, Optimum Design Methods in Aerodynamics*. von Karman Institute for Fluid Dynamics, 1994.
16. J. Reuther, A. Jameson, J. J. Alonso, M. J. Rimlinger, and D. Saunders. Constrained multipoint aerodynamic shape optimization using an adjoint formulation and parallel computers. *AIAA paper 97-0103*, 35th Aerospace Sciences Meeting and Exhibit, Reno, Nevada, January 1997.
17. J. Reuther, J. J. Alonso, J. C. Vassberg, A. Jameson, and L. Martinelli. An efficient multiblock method for aerodynamic analysis and design on distributed memory systems. *AIAA paper 97-1893*, June 1997.
18. O. Baysal and M. E. Eleshaky. Aerodynamic design optimization using sensitivity analysis and computational fluid dynamics. *AIAA Journal*, 30(3):718–725, 1992.
19. J.C. Huan and V. Modi. Optimum design for drag minimizing bodies in incompressible flow. *Inverse Problems in Engineering*, 1:1–25, 1994.
20. M. Desai and K. Ito. Optimal controls of Navier-Stokes equations. *SIAM J. Control and Optimization*, 32(5):1428–1446, 1994.
21. W. K. Anderson and V. Venkatakrishnan. Aerodynamic design optimization on unstructured grids with a continuous adjoint formulation. *AIAA paper 97-0643*, 35th Aerospace Sciences Meeting and Exhibit, Reno, Nevada, January 1997.
22. J. Elliott and J. Peraire. 3-D aerodynamic optimization on unstructured meshes with viscous effects. *AIAA paper 97-1849*, June 1997.
23. S. Ta'asan, G. Kuruvila, and M. D. Salas. Aerodynamic design and optimization in one shot. *AIAA paper 92-0025*, 30th Aerospace Sciences Meeting and Exhibit, Reno, Nevada, January 1992.
24. A. Jameson, L. Martinelli, and J. Vassberg. Reduction of the adjoint gradient formula in the continuous limit. *AIAA paper*, 41<sup>st</sup> AIAA Aerospace Sciences Meeting, Reno, NV, January 2003.
25. A. Jameson and J.C. Vassberg. Studies of alternative numerical optimization methods applied to the brachistochrone problem. *Computational Fluid Dynamics*, 9:281–296, 2000.
26. A. Jameson, W. Schmidt, and E. Turkel. Numerical solutions of the Euler equations by finite volume methods with Runge-Kutta time stepping schemes. *AIAA paper 81-1259*, January 1981.
27. L. Martinelli and A. Jameson. Validation of a multigrid method for the Reynolds averaged equations. *AIAA paper 88-0414*, 1988.
28. S. Tatsumi, L. Martinelli, and A. Jameson. A new high resolution scheme for compressible viscous flows with shocks. *AIAA paper To Appear*, AIAA 33rd Aerospace Sciences Meeting, Reno, Nevada, January 1995.
29. A. Jameson. Optimum aerodynamic design using control theory. *Computational Fluid Dynamics Review*, pages 495–528, 1995.
30. A. Jameson, Sriram, and L. Martinelli. An unstructured adjoint method for transonic flows. *AIAA paper*, 16<sup>th</sup> AIAA CFD Conference, Orlando, FL, June 2003.
31. E. Ahlstorm, R. Gregg, J. Vassberg, and A. Jameson. The design of an unlimited class reno racer. *AIAA paper-4341*, 18<sup>th</sup> AIAA Applied Aerodynamics Conference, Denver, CO, August 2000.
32. A. Jameson and L. Martinelli. Aerodynamic shape optimization techniques based on control theory. Lecture notes in mathematics #1739, proceeding of computational mathematics driven by industrial problems, CIME (International Mathematical Summer (Center), Martina Franca, Italy, June 21-27 1999.

### COMPARISON OF CHORDWISE PRESSURE DISTRIBUTIONS B747 WING-BODY

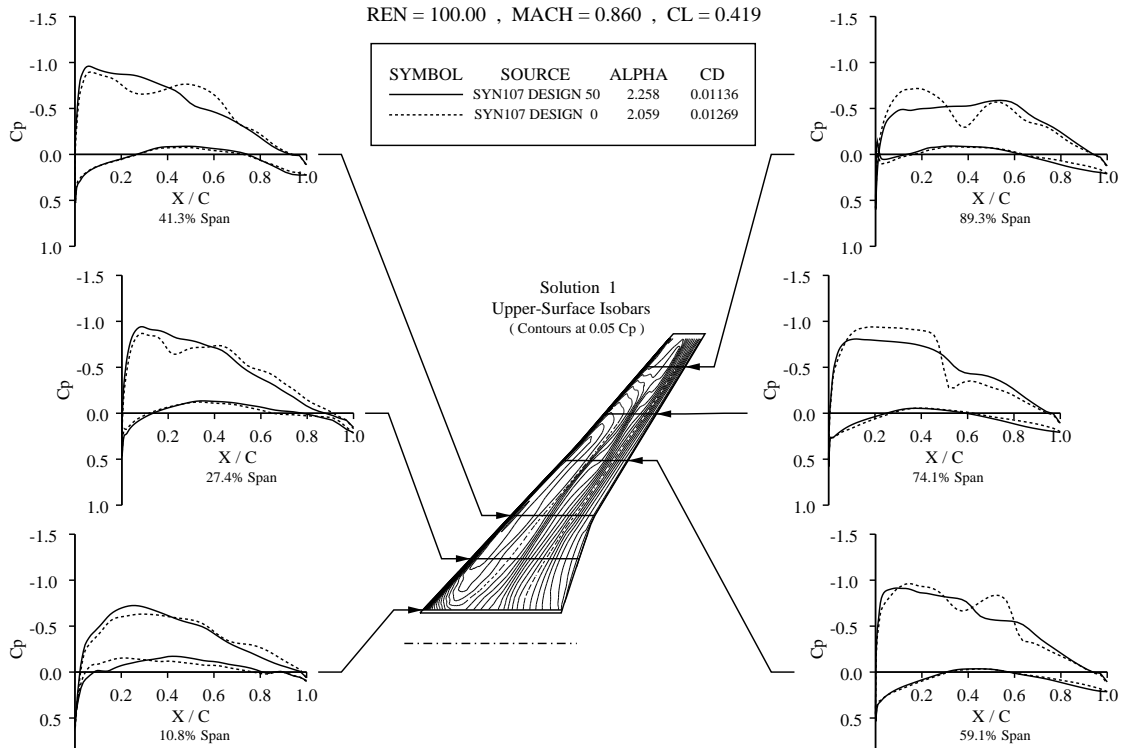


Fig. 2. Redesigned Boeing 747 wing at Mach 0.86, Cp distributions

### COMPARISON OF CHORDWISE PRESSURE DISTRIBUTIONS B747 WING-BODY

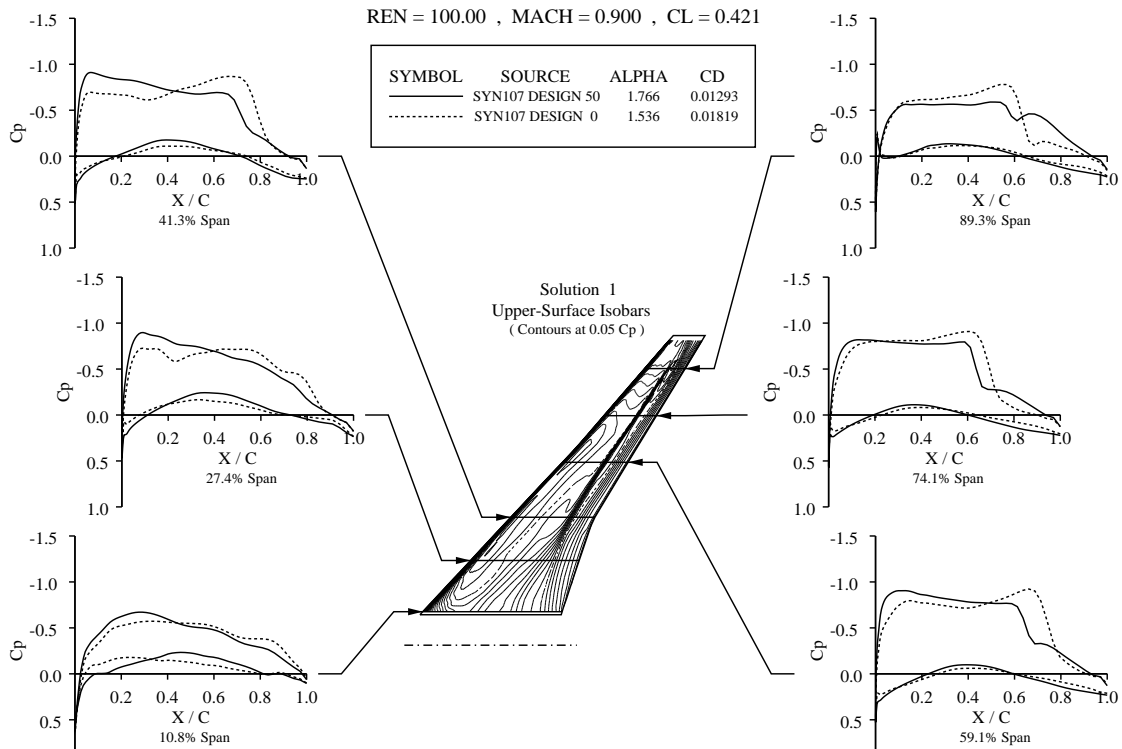
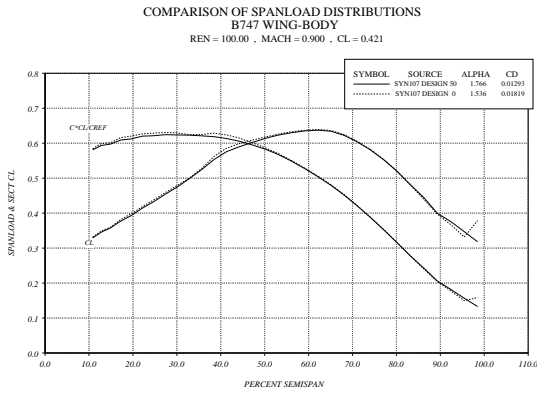
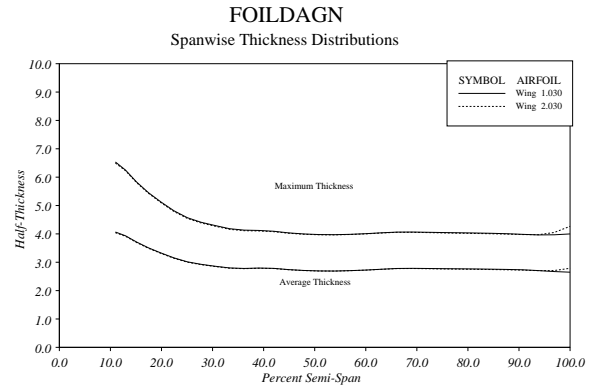


Fig. 3. Redesigned Boeing 747 wing at Mach 0.90, Cp distributions



**Fig. 4.** Span loading, Redesigned Boeing 747 wing at Mach 0.90



**Fig. 5.** Spanwise thickness distribution, Redesigned Boeing 747 wing at Mach 0.90

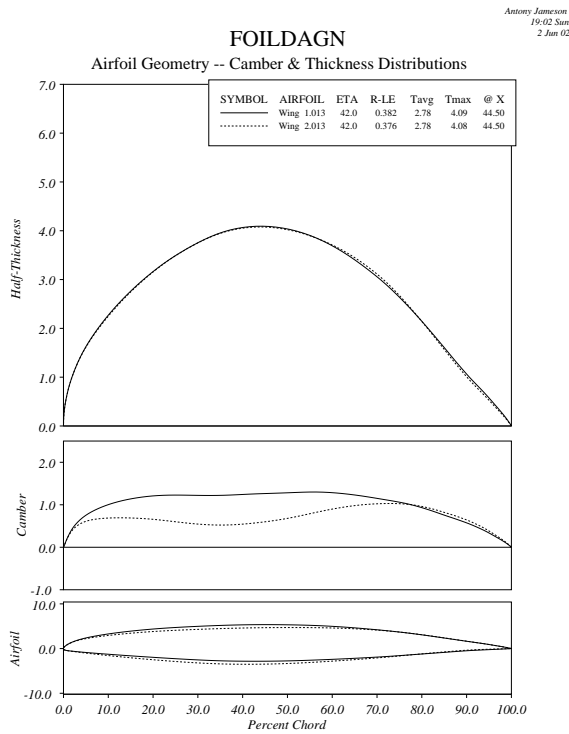


**Fig. 6.** Section geometry at  $\eta = 0.42$ , redesigned Boeing 747 wing at Mach 0.90

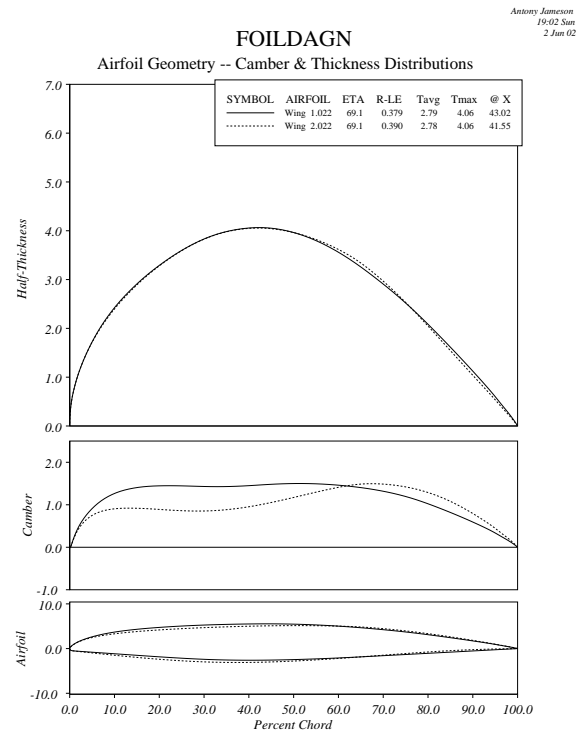


**Fig. 7.** Section geometry at  $\eta = 0.68$ , redesigned Boeing 747 wing at Mach 0.90

Mach: 0.840 Alpha: 3.060  
 CL: 0.325 CD: 0.02319 CM: 0.0000  
 Design: 0 Residual: 0.2763E-02  
 Grid: 193X 33X 33

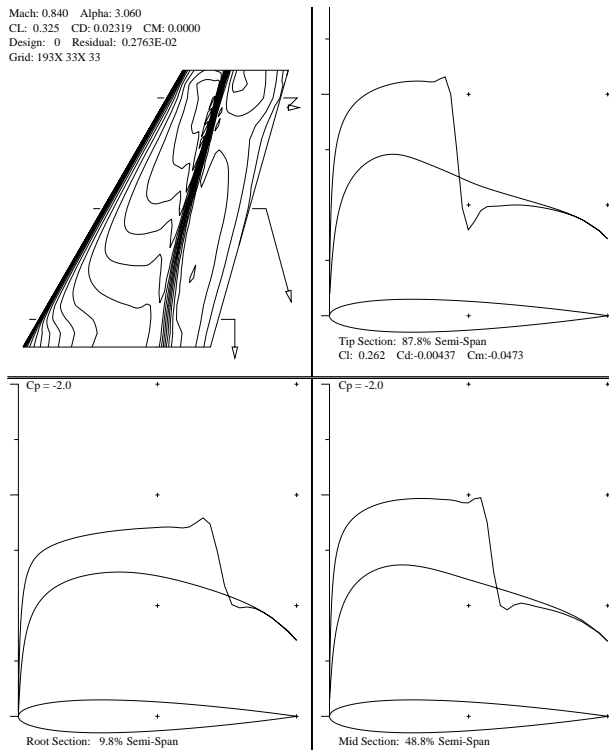


**Fig. 8.** Initial pressure distribution over a NACA 0012 wing

Mach: 0.840 Alpha: 3.060  
 CL: 0.314 CD: 0.01592 CM: 0.0000  
 Design: 50 Residual: 0.1738E+00  
 Grid: 193X 33X 33

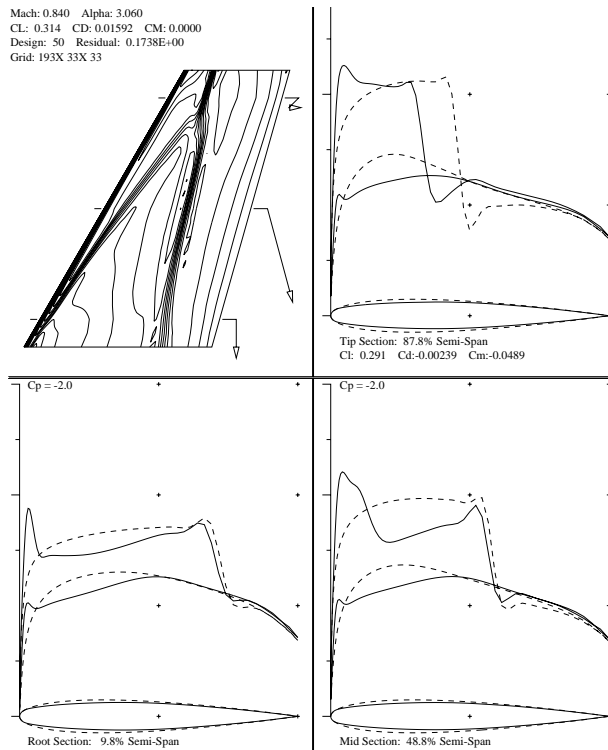


**Fig. 9.** Final pressure distribution and modified section geometries along the wing span

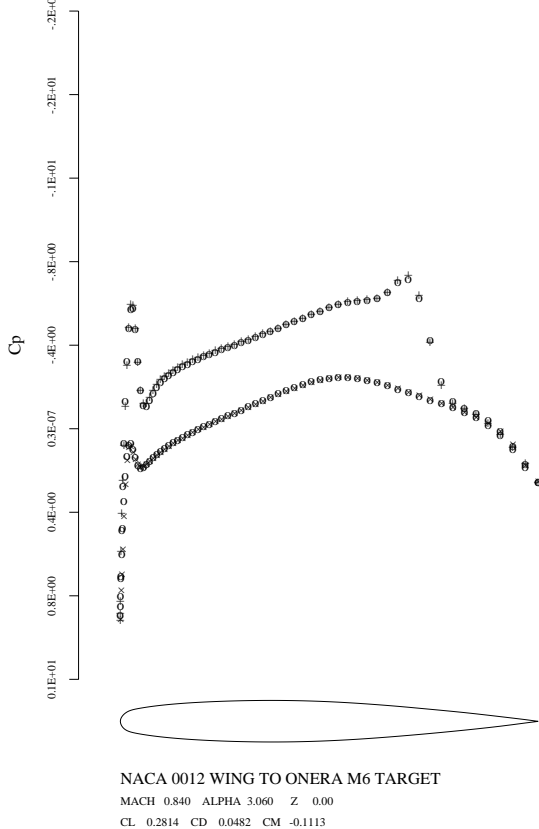


**Fig. 10.** Final computed and target pressure distributions at 0 % of the wing span

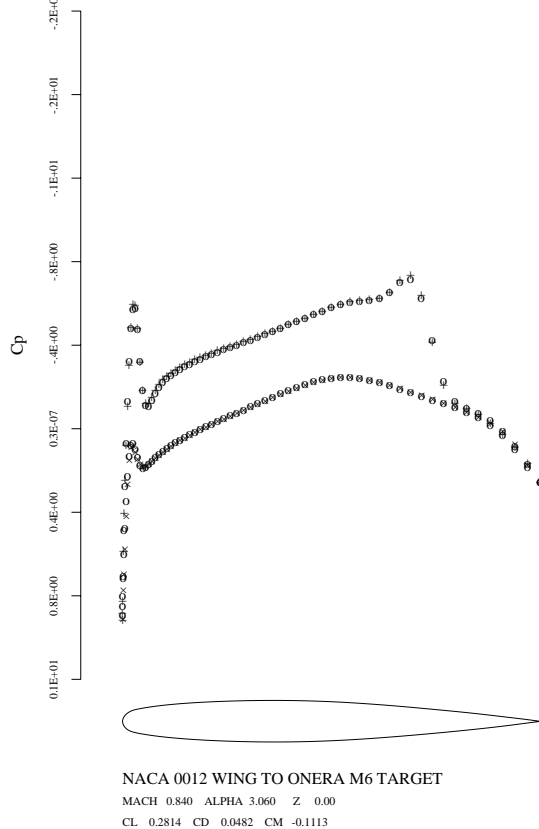


**Fig. 11.** Final computed and target pressure distributions at 20 % of the wing span

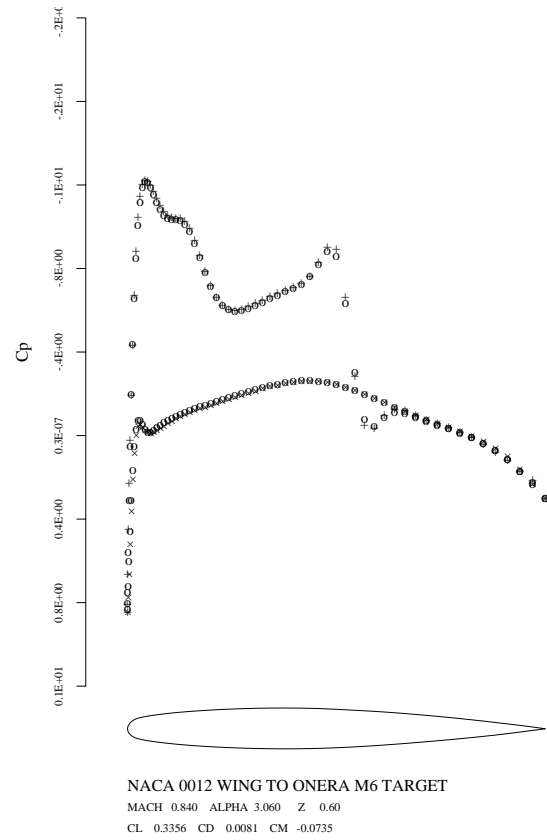
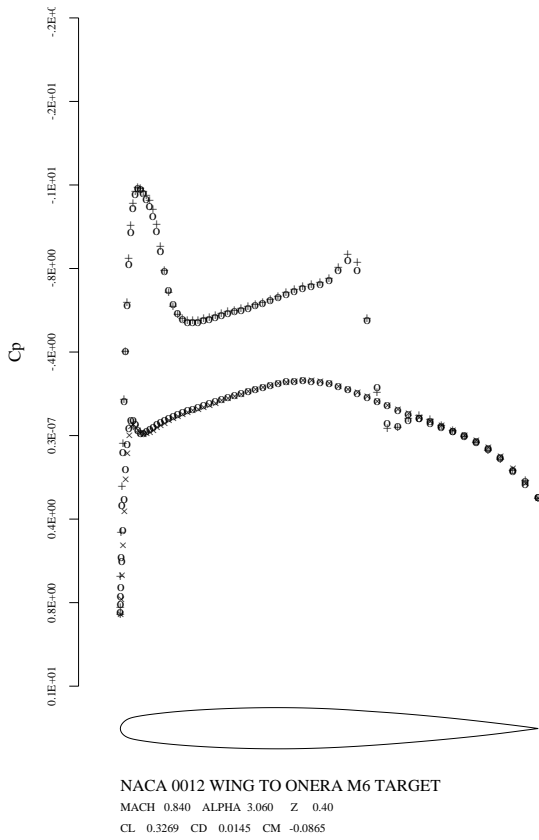


**Fig. 12.** Final computed and target pressure distributions at 40 % of the wing span

**Fig. 13.** Final computed and target pressure distributions at 60 % of the wing span

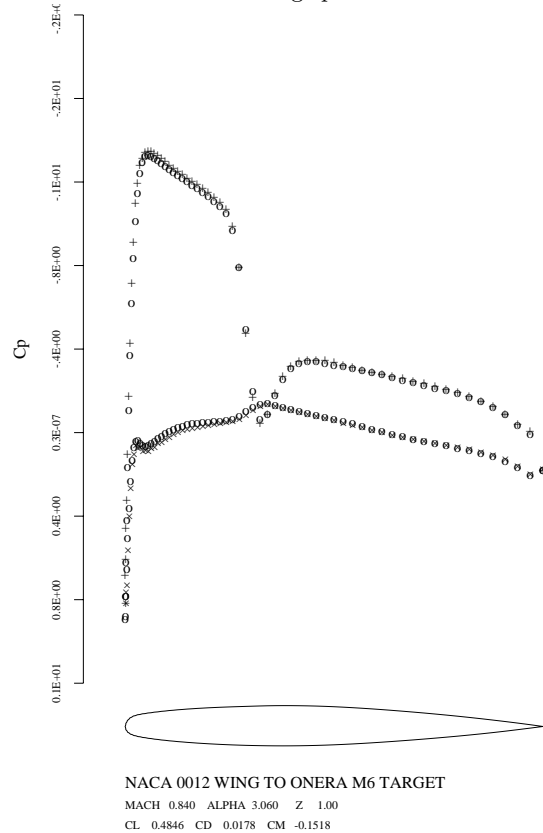
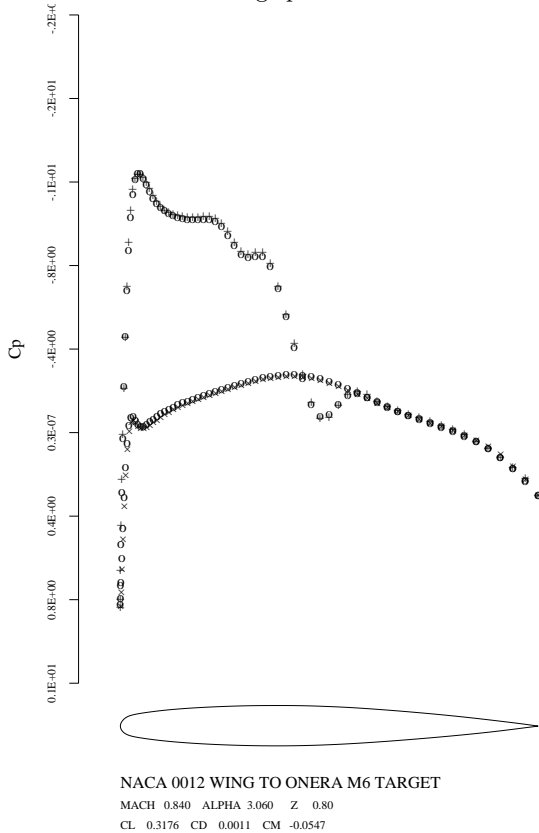


**Fig. 14.** Final computed and target pressure distributions at 80 % of the wing span

**Fig. 15.** Final computed and target pressure distributions at 100 % of the wing span

Mach: 0.780 Alpha: 1.400  
 CL: 0.280 CD: 0.00624 CM: 0.0000  
 Design: 60 Residual: 0.1528E+00  
 Grid: 193X 33X 49

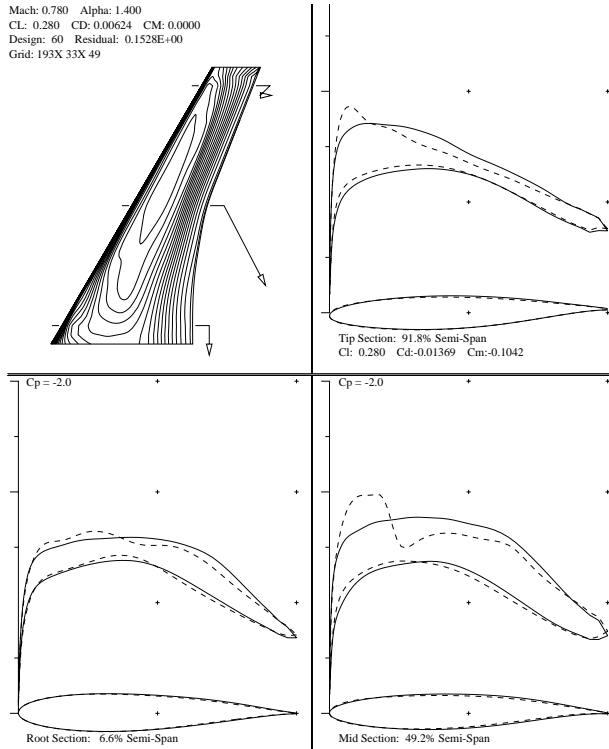
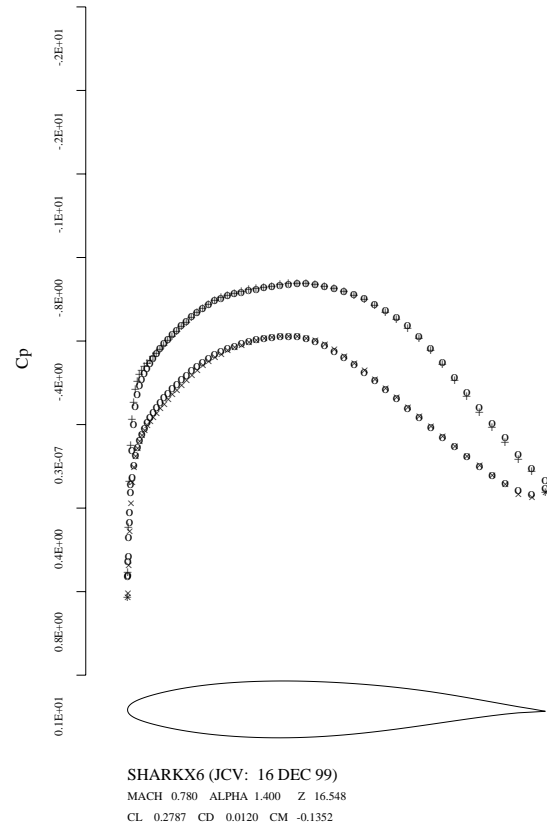
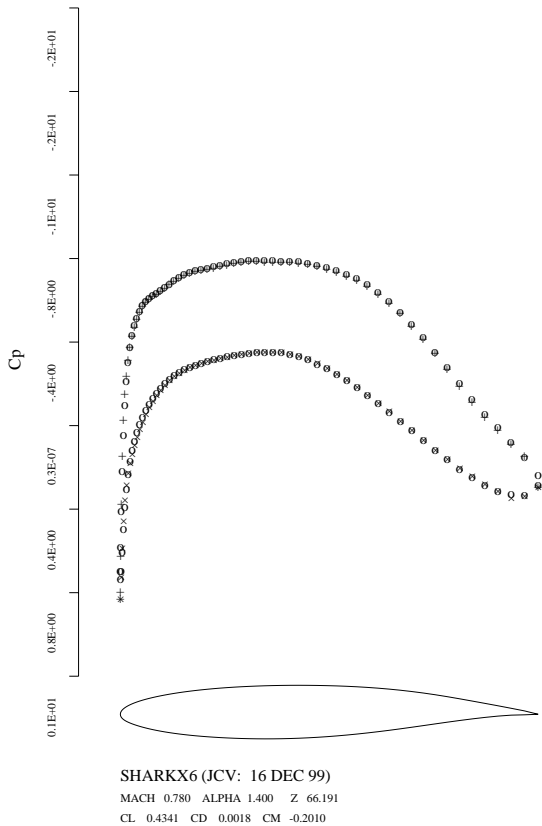


**Fig. 16.** Initial and final pressure and section geometries



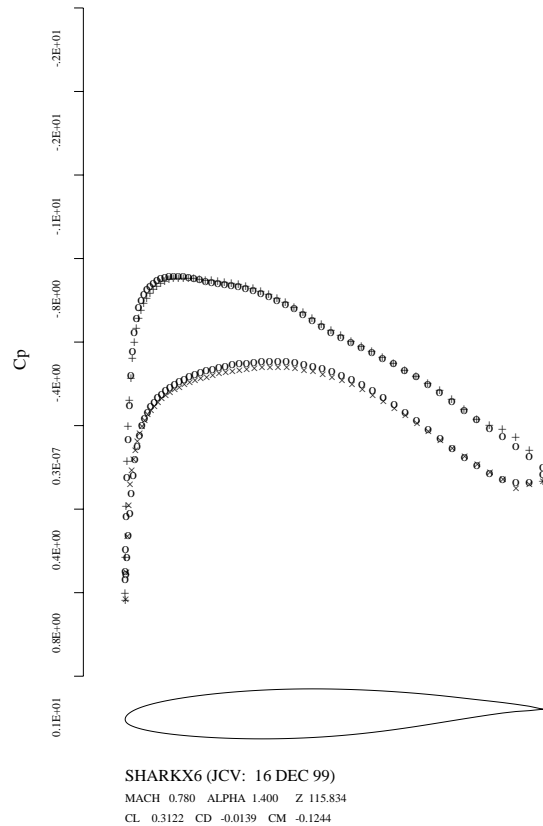
SHARKX6 (JCV: 16 DEC 99)  
 MACH 0.780 ALPHA 1.400 Z 16.548  
 CL 0.2787 CD 0.0120 CM -0.1352

**Fig. 17.** Initial and final pressure distributions at 5 % of the wing span



SHARKX6 (JCV: 16 DEC 99)  
 MACH 0.780 ALPHA 1.400 Z 66.191  
 CL 0.4341 CD 0.0018 CM -0.2010

**Fig. 18.** Initial and final pressure distributions at 50 % of the wing span



SHARKX6 (JCV: 16 DEC 99)  
 MACH 0.780 ALPHA 1.400 Z 115.834  
 CL 0.3122 CD -0.0139 CM -0.1244

**Fig. 19.** Initial and final pressure distributions at 95 % of the wing span

Mach: 0.780 Alpha: 1.421  
CL: 0.279 CD: 0.00613 CM:-1.2454  
Design: 10 Residual: 0.1887E-01  
Grid: 193X 33X 49

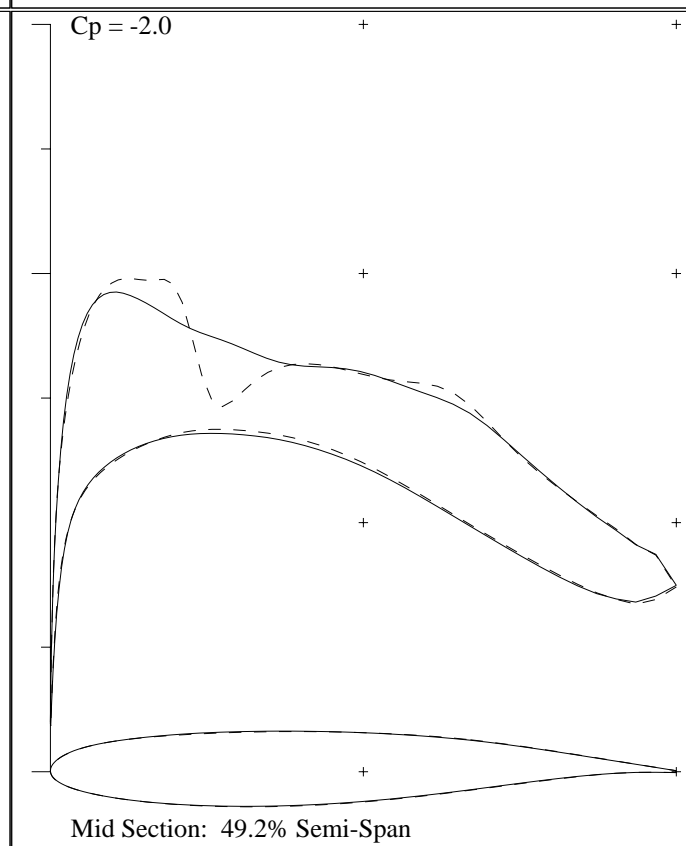
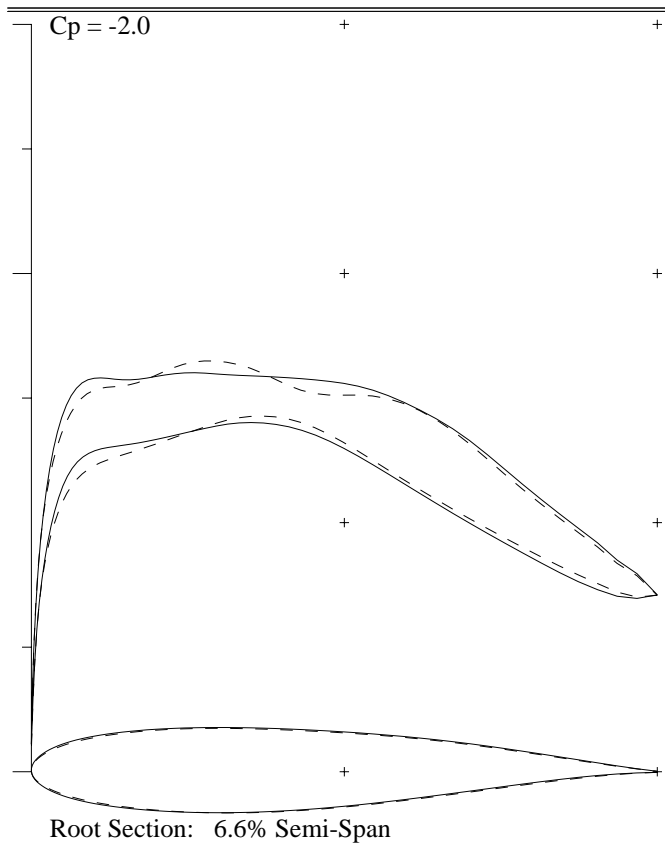
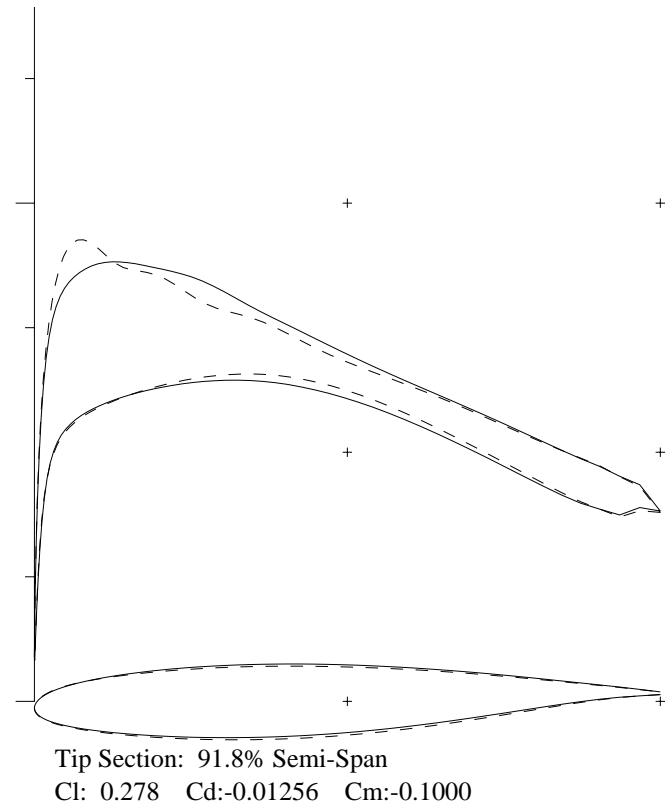
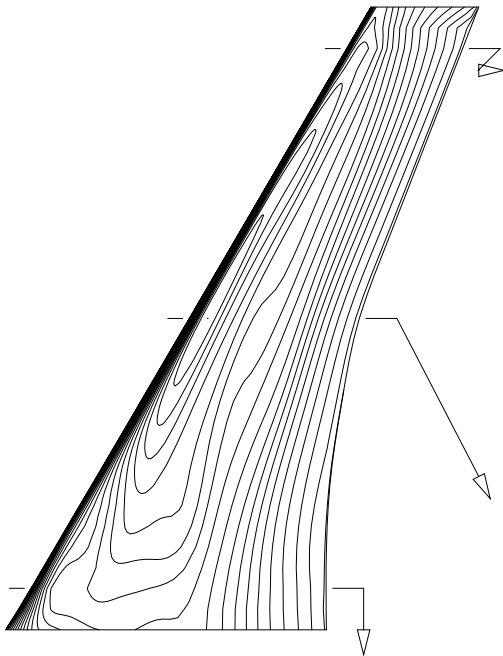


Fig. 20. Drag minimization for the SHARK wing